CHAPTER

4

The Subsurface Environment

Petroleum geology is largely concerned with the study of fluids, not just the oil and gas discussed in Chapter 2, but the waters with which they are associated and through which they move. Before examining the generation and migration of oil and gas in Chapter 5, the subsurface environment in which these processes operate should be considered.

This chapter begins with an account of subsurface waters, and then considers pressure and temperature and their effects on the condensation and evaporation of gas and oil. The chapter concludes by putting these ingredients together and discussing the dynamics of fluids in basins.

4.1 SUBSURFACE WATERS

Two types of water can be recognized in the subsurface by their mode of occurrence:

1. Free water
2. Interstitial, or irreducible, water

Free water is free to move in and out of pores in response to a pressure differential. Interstitial water, on the other hand, is bonded to mineral grains, both by attachment to atomic lattices as hydroxyl radicals, and as a discrete film of water. Interstitial water is often referred to as *irreducible water* because it cannot be removed during the production of oil or gas from a reservoir.

4.1.1 Analysis

Subsurface waters are analyzed for several specific reasons, apart from general curiosity. As discussed in Chapter 3, the measurement of the resistivity of formation water (R_w) is essential for the accurate assessment of S_w, and hence hydrocarbon saturation. Of course, R_w is closely related to salinity. Salinity varies both vertically and laterally across a basin. Salinity often increases with proximity to hydrocarbon reservoirs. Therefore, regional salinity maps may be an important exploration tool. Similarly, subsurface waters contain traces of dissolved hydrocarbon gases, whose content increases with proximity to hydrocarbon accumulations.

Subsurface waters can be analyzed in two ways. The total concentration of solids, or salinity, can be calculated from R_w by using the S.P. log, as discussed in Chapter 3.

Elements of Petroleum Geology
http://dx.doi.org/10.1016/B978-0-12-386031-6.00004-7

Alternatively, samples can be obtained from drill stem tests or during production. Care has to be taken when interpreting samples from drill stem tests because of the likelihood of contamination by mud filtrate.

4.1.2 Genesis

Traditionally, four types of subsurface water can be defined according to their genesis:

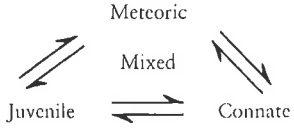

Meteoric waters occur near the earth's surface and are caused by the infiltration of rainwater. Their salinity, naturally, is negligible, and they tend to be oxidizing. Meteoric waters are often acidic because of dissolved humic, carbonic, and nitrous acid (from the atmosphere), although they may quickly become neutralized in the subsurface, especially when they flow through carbonate rocks. Connate waters are harder to define. They were originally thought of as residual seawater that was trapped during sedimentation. Current definitions proposed for connate waters include "interstitial water existing in the reservoir rock prior to disturbance by drilling" (Case, 1956) and "waters which have been buried in a closed hydraulic system and have not formed part of the hydraulic cycle for a long time" (White, 1957). Connate waters differ markedly from seawater both in concentration and chemistry.

Juvenile waters are of primary magmatic origin. It may be difficult to prove that such hydrothermal waters are indeed primary and have received no contamination whatsoever from connate waters. These three definitions lead naturally to the fourth class of subsurface waters—those of mixed origin. The mixed waters may be caused by the confluence of juvenile, connate, or meteoric waters. In most basins a transition zone exists between the surface aquifer and the deeper connate zone. The effect of this transition zone on the S.P. curve was discussed in Chapter 3.

4.1.3 Chemistry of Subsurface Waters

The four characteristics of subsurface water to consider are Eh, pH, concentration, and composition.

4.1.3.1 Eh and pH

The current data on the Eh and pH of subsurface waters are summarized in Fig. 4.1 (see Krumbein and Garrels (1952), Pirson (1983), Friedman and Sanders (1978)). The data show that rainwater is oxidizing and acidic. It generally contains oxygen, nitrogen, and carbon dioxide in solution, together with ammonium nitrate after thunderstorms.

As rainwater percolates into the soil it undergoes several changes as it becomes meteoric water. It tends to become reducing as it oxidizes organic matter. The pH of meteoric water may remain low in swampy environments because of the humic acids, but it increases in arid climates. If meteoric waters flow deep into the subsurface, they gradually dissolve salts

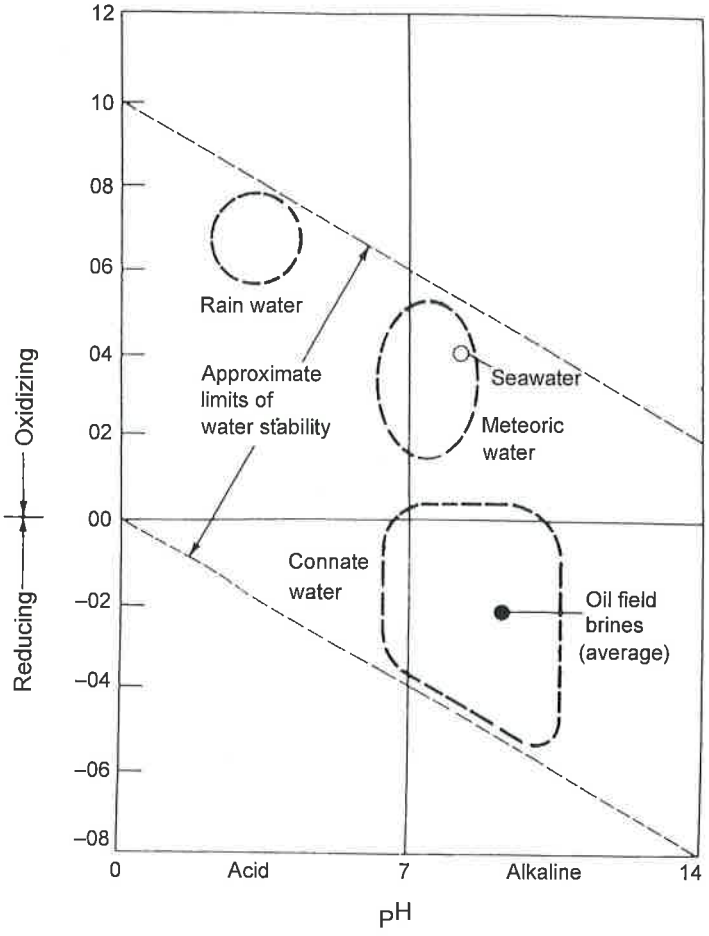

FIGURE 4.1 Oxidation:reduction potential–pH graph showing the approximate distribution of the various types of subsurface fluid.

and increase in pH. Deep connate waters show a wide range of Eh and pH values depending on their history, and particularly on the extent to which they have mixed with meteoric waters or contain paleoaquifers trapped beneath unconformities.

Oil field brines tend to be alkaline and strongly reducing. For further details on the Eh of subsurface fluids and its significance in petroleum exploration, see Pirson (1983). The Eh and pH of pore fluids control the precipitation and solution of clays and other diagenetic mineral cements. Obviously, the study of their relationship with diagenesis and porosity evolution is important, and is discussed in Chapter 6 in further detail.

4.1.3.2 *Concentration*

The significance of measuring the concentration of salts in subsurface waters has already been mentioned. Not only is it important for well evaluation, but the data may be plotted

regionally as an exploration tool. Salinity or, more properly, the total of dissolved solids, is measured in parts per million, but is more conveniently expressed in milligrams per liter:

$$\text{mg/l} = \frac{\text{ppm}}{\text{density}}.$$

Average seawater has approximately 35,000 ppm (3.5%) of dissolved minerals. Values in subsurface waters range from about 0 ppm for fresh meteoric waters up to 642,798 ppm for a brine from the Salina dolomite of Michigan (Case, 1956). The latter value is extremely high because of solution from evaporites. In most connate waters the dissolved solids content seldom exceeds 350,000 ppm. In sands the salinity of connate waters generally increases with depth (Fig. 4.2) at rates ranging from 80 to 300 mg/l m (Dickey, 1979). For sources of data, see Dickey (1966, 1969) and Russell (1951).

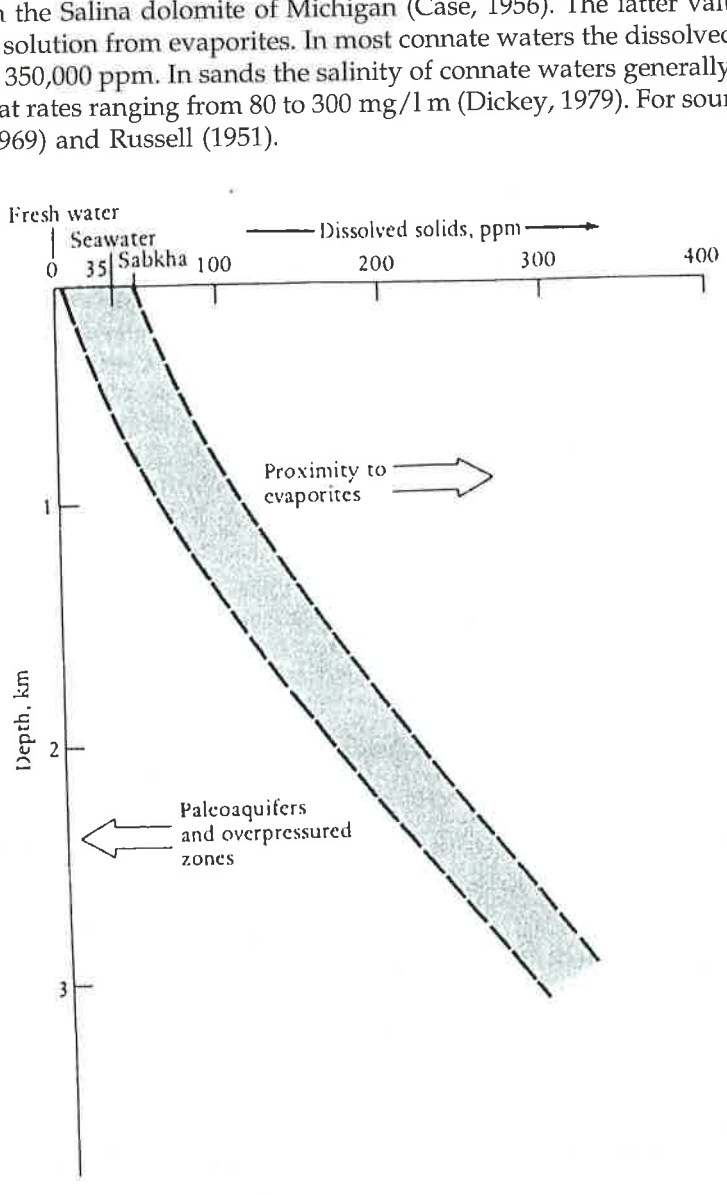

FIGURE 4.2 Graph of salinity against depth for subsurface waters. *After Dickey (1966, 1969), Russell (1951).*

Local reversals of this general trend have been seen and are attributable to two causes. Meteoric water may sometimes be trapped beneath an unconformity and is thus preserved as a paleoaquifer. A noted example of this occurrence has been documented from the sub-Cretaceous unconformity of Israel (Bentor, 1969). Here the beds above the unconformity have salinities of 60,000 ppm. The salinity drops to approximately 20,000 ppm beneath the unconformity before gradually increasing again with depth to more than 40,000 ppm.

Similarly in the North Sea there is good evidence that Cretaceous rainwater still lies, with little modification, as a paleoaquifer in Jurassic sands truncated by the Cimmerian unconformity (Macaulay et al., 1992). Reversals of increasing salinity with depth are also noted in zones of overpressure. This phenomenon is discussed in more detail later, but basically it reflects the fact that overpressured waters are trapped and cannot circulate. In shales, however, the increase in salinity with depth is less marked. The salinity of sand is often about three times that of the shales with which it may be interbedded (Dickey, 1979). This difference, together with the overall increase in salinity with depth, has been attributed to salt sieving (De Sitter, 1947). Shales may behave like semipermeable membranes. As water moves upward through compacting sediments, the shale prevents the salt ions from escaping from the sands, with the net result that salinity increases progressively with depth (see Magara (1977, 1978), for further details). Based on studies in the Gulf of Mexico and the Mackenzie Delta, Overton (1973) and Van Elsberg (1978) have defined four major subsurface environments:

Zone 1: Surface, depth of about 1 km; zone of circulating meteoric water. Salinity is fairly uniform.
Zone 2: Depth of about 1–3 km; salinity gradually increases with depth. Saline formation water is ionized (Fig. 4.2).
Zone 3: Depth greater than 3 km; chemically reducing environment in which hydrocarbons form. Salinity is uniform with increasing depth; may even decline if overpressured.
Zone 4: Incipient metamorphism with recrystallization of clays to micas.

Having finished our discussion of vertical salinity variations, it is now appropriate to consider lateral salinity changes. Salinity has long been known to tend to increase from the margins of a basin toward its center. Figure 4.3 illustrates a regional salinity map for the Mississippian Madison limestone aquifer in the Williston Basin of North Dakota and surrounding areas. Many instances of this salinity increase have been documented (Case, 1945; Youngs, 1975). This phenomenon is easy to explain: The basin margins are more susceptible to circulating meteoric water than is the basin center, where flow is negligible or coming from below. Regional isohaline maps can be a useful exploration tool, indicating areas of anomalously high salinity. These areas are presumably stagnant regions unaffected by meteoric flow, where oil and gas accumulations may have been preserved.

4.1.3.3 *Composition*

Subsurface waters contain varying concentrations of inorganic salts together with traces of organic compounds, including hydrocarbons. Table 4.1 presents analyses of many subsurface waters. For additional data, see Krejci-Graf (1962, 1978) and Collins (1975).

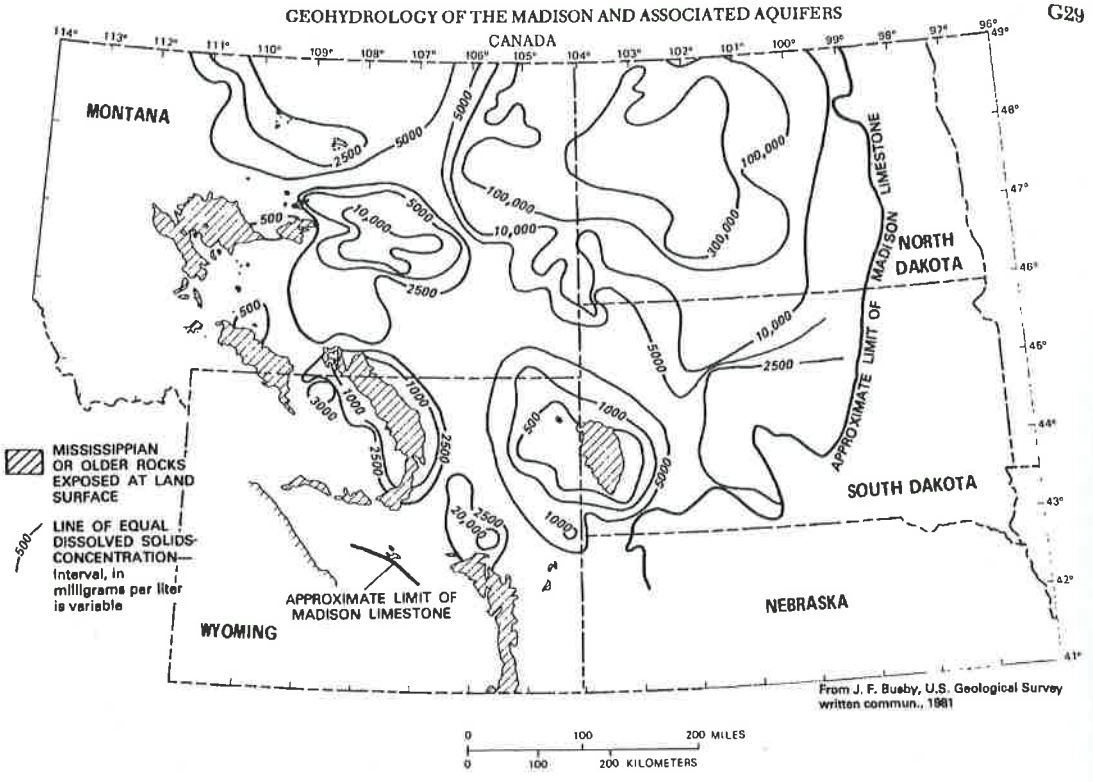

FIGURE 4.3 Regional salinity map for the Mississippian Madison limestone aquifer in the Williston Basin. Contour values are in parts per million of total dissolved solids; contour interval is variable. *From Downey (1984).*

Meteoric waters differ from connate waters not only in salinity but also in chemistry. Meteoric waters have higher concentrations of bicarbonate and sulfate ions and lower amounts of calcium and magnesium. These differences are the basis for the classification of subsurface waters proposed by Sulin (1946), which has been widely adopted by geologists (Table 4.2). For reviews of this classification and others, see Ostroff (1967).

Connate waters differ from seawater not only because they contain more dissolved solids but also in their chemistry. Connate waters contain a lower percentage of sulfates, magnesium, and often calcium (possibly caused by the precipitation of anhydrite, dolomite, and calcite) and a higher percentage of sodium, potassium, and chlorides than does seawater.

Because of the complex composition of subsurface waters, they can best be displayed and compared graphically. Schemes have been proposed by Tickell (1921) and Sulin (1946). The composition of seawater and typical connate waters are plotted according to these schemes in Fig. 4.4.

Connate waters also contain traces of dissolved hydrocarbons. The seminal work on this topic was published by Buckley et al. (1958). Basing their work on a study of hundreds of drill stem tests from the Gulf Coast, they found methane dissolved in subsurface waters at

TABLE 4.1 Representative Oil Field Water Analyses (ppm)

Pool	Reservoir rock, age	Cl^-	SO_4^-	CO_3^-	HCO_3^-	$Na^+ + K^+$	Ca^{2+}	Mg^{2+}	Total (ppm)
Seawater, ppm		19,350	2690	150		11,000	420	1300	35,000
Seawater, %		55.3	7.7	0.2		31.7	1.2	3.8	
Lagunillas, Western Venezuela	2000–3000 ft, Miocene	89	—	120	5263	2003	10	63	7548
Conroe, Texas	Conroe sands, Eocene	47,100	42	288		27,620	1865	553	77,468
East Texas	Woodbine sand, Upper Cretaceous	40,598	259	387		24,653	1432	335	68,964
Burgan, Kuwait	Sandstone, Cretaceous	95,275	198	—	360	46,191	10,158	2206	154,388
Rodessa, Texas, LA	Oolitic limestone, Lower Cretaceous	140,063	284	—	73	61,538	20,917	2874	225,749
Davenport, OK	Prue sand, Pennsylvanian	119,855	132	—	122	62,724	9977	1926	194,736
Bradford, PA	Bradford sand, Devonian	77,340	730	—	—	32,600	13,260	1940	125,870
Oklahoma City, OK	Simpson sand, Ordovician	184,387	286	—	18	91,603	18,753	3468	298,497
Garber, OK	Arbuckle limestone, Ordovician	139,496	352	—	43	60,7333	21,453	2791	224,868

From Geology of Petroleum by Leworsen. © 1967 by W. H. Freeman and Company. Used with permission.

concentrations of up to 14 standard cubic feet per barrel. They also recorded ethane and propane and very minor concentrations of heavier hydrocarbons. The amount of dissolved gases correlated with salinity, increasing with depth and from basin margin to center. Halos of gas-enriched connate waters were recorded around oil fields.

TABLE 4.2 Major Classes of Water by Sulin Classification

	Ratios of concentrations, expressed as milliequivalent percent		
Types of water (V. A. Sulin)	$\frac{Na}{Cl}$	$\frac{Na-Cl}{So_4}$	$\frac{Cl-Na}{Mg}$
Meteoric			
Sulfate-sodium	>1	<1	<0
Bicarbonate-sodium	>1	>1	<0
Connate			
Chloride-magnesium	<1	<0	<1
Chloride-calcium	<1	<0	>1

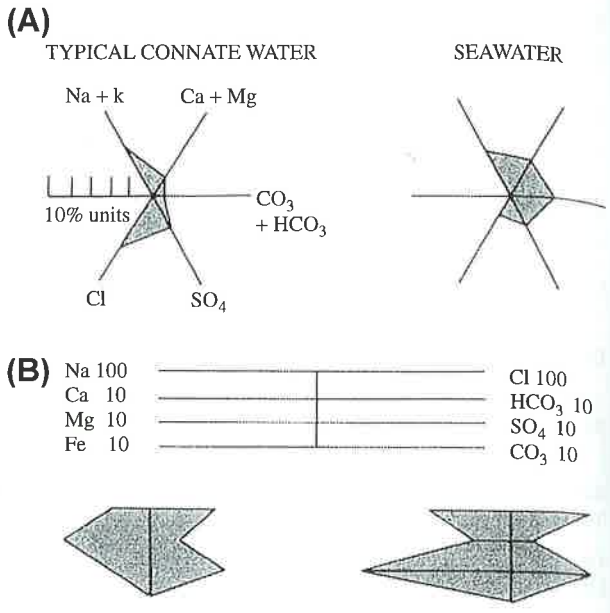

FIGURE 4.4 Methods of plotting water chemistry. (A) Tickell plots and (B) Sulin plots for a typical connate water sample (left) and seawater (right).

These data are of great significance for two reasons. They raise the possibility of regionally mapping dissolved gas content as a key to locating new oil and gas fields. These data also have some bearing on the problems of the migration of oil and gas (for an example, see Price (1980)). This topic is discussed in more detail in Chapter 5.

4.2 SUBSURFACE TEMPERATURES

4.2.1 Basic Principles

Temperature increases from the earth's surface toward its center. Bottom hole temperatures (BHTs) can be recorded from wells and are generally taken several times at each casing point. As each log is run, the BHT can be measured. It is important to take several readings at each depth because the mud at the bottom of the hole takes hours to warm up to the ambient temperature of the adjacent strata. Thus BHTs are recorded together with the number of hours since circulation. Figure 4.5 shows a BHT buildup curve. The true stabilized temperature can be determined from the Horner plot (Fertl and Wichmann, 1977). In this method the recorded temperature is plotted against the following ratio:

$$\frac{\Delta t}{(t + \Delta t)},$$

where Δt = number of hours since circulation and logging and t = hours of circulation at that depth. An example of a Horner plot is shown in Fig. 4.6. For a more detailed analysis of this topic, see Carstens and Finstad (1981).

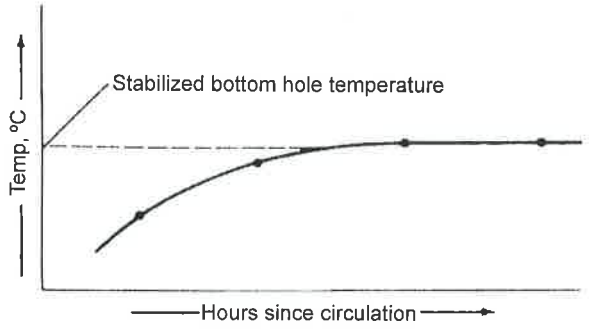

FIGURE 4.5 Graph showing how true BHT can only be determined from several readings taken many hours apart.

Once several corrected BHTs have been obtained as a well is drilled, they can be plotted against depth to calculate the geothermal gradient (Fig. 4.7). These values range from approximately 1.8 to 5.5 °C/100 m. The global average is about 2.6 °C/100 m. When several BHTs are plotted against depth for a well they may show that the geothermal gradient is not constant with depth. This discrepancy is generally caused by variations in the thermal conductivity of the penetrated strata. This relationship may be expressed as follows:

Table 4.3 shows the thermal conductivity of various sediments. Where sediments of different thermal conductivity are interbedded, the geothermal gradient will be different for each formation.

$$\text{Heat flow} = \text{geothermal gradient} \times \text{thermal conductivity of rock.}$$

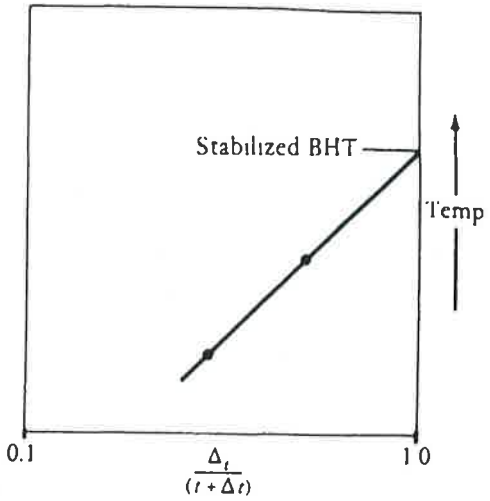

FIGURE 4.6 Horner plot showing how true BHT can be extrapolated from two readings.

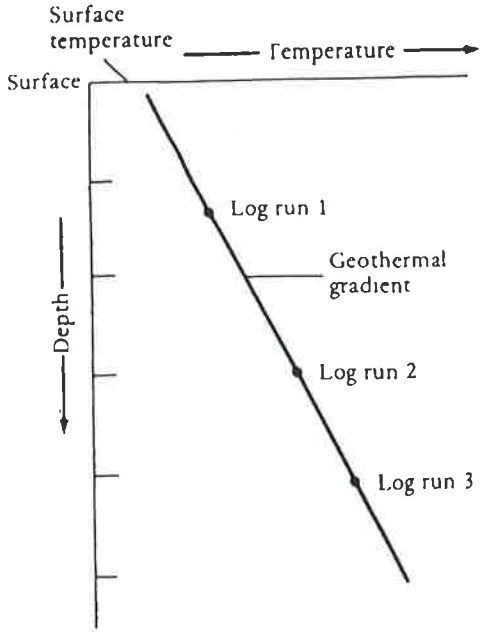

FIGURE 4.7 Sketch showing how geothermal gradient may be determined from two or more BHTs taken at different log runs.

A wide range of values can be expected for sands, shales, and limestones because of porosity variations. Because thermal conductivity is lower for water than it is for minerals, it increases with decreasing porosity and increasing depth of burial according to the following formula:

$$K_{pr} = K_w^{\Phi}, \; K_r^{1\Phi},$$

TABLE 4.3 Thermal Conductivity of Various Rocks

Lithology	Thermal conductivity (W/m °C)
Halite	5.5
Anhydrite	5.5
Dolomite	5.0
Limestone	2.8–3.5
Sandstone	2.6–4.0
Shale	1.5–2.9
Coal	0.3

From Evans (1977), Oxburgh and Andrews-Speed (1981).

where

K_{pr} = bulk saturated conductivity
K_w = conductivity of pore fluid
K_r = conductivity of the rock at zero porosity
Φ = porosity

Figure 4.8 illustrates the vertical variations in conductivity, porosity, and geothermal gradient for a well in the North Sea. Note how conductivity increases and gradient decreases with depth and declining porosity. Local vertical variations are due to lithology, especially the high thermal conductivity of the Zechstein evaporites.

Once the geothermal gradient is established, isotherms can be drawn (Fig. 4.9). Note that the vertical spacing of isotherms decreases with conductivity and increasing geothermal gradient.

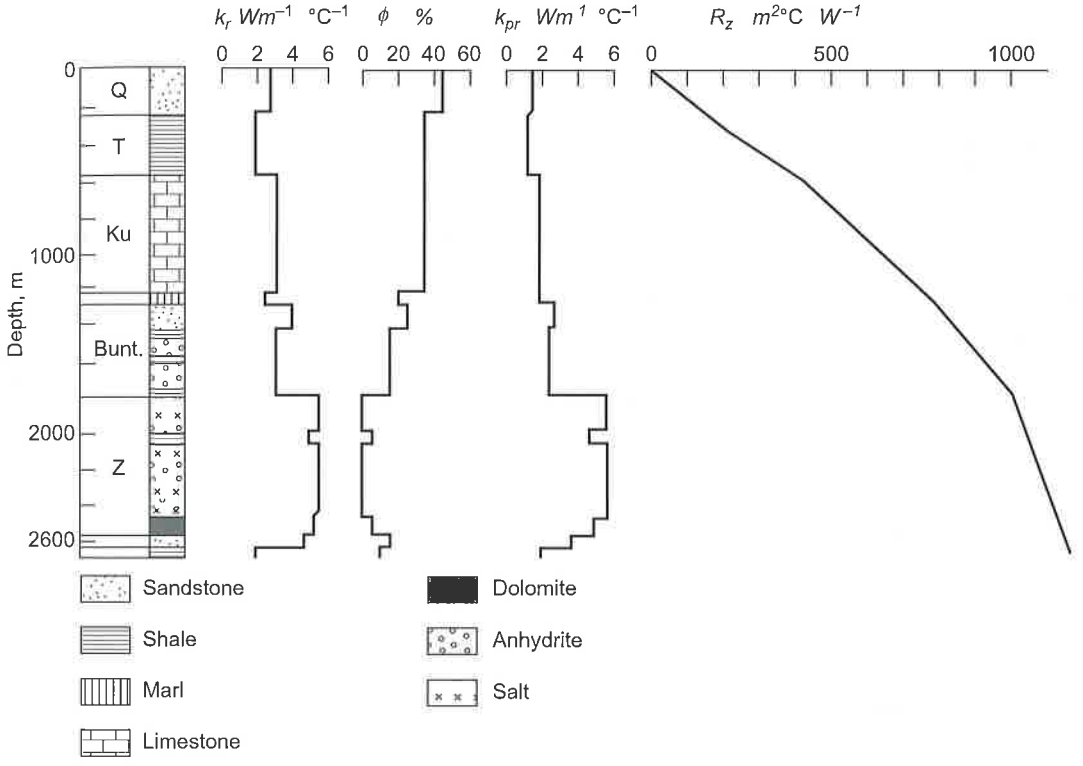

FIGURE 4.8 Variations in thermal conductivity, porosity, and geothermal gradient for a well in the North Sea. Note how thermal conductivity and gradient gradually increase with depth and declining porosity. Note also the local fluctuations due to lithology, especially the high conductivity of the Zechstein evaporites. *After Oxburgh and Andrews-Speed (1981).*

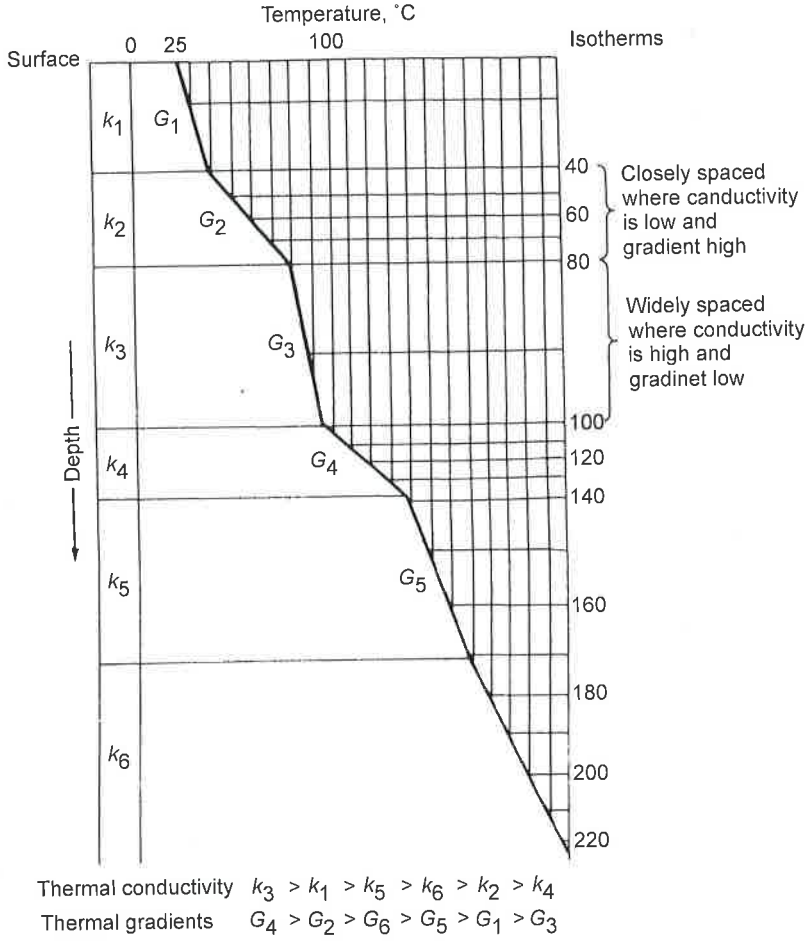

FIGURE 4.9 Depth–temperature plot showing the effect of rocks of differing thermal conductivity (K) on geothermal gradient (G) and the vertical spacing of isotherms.

4.2.2 Local Thermal Variations

Once the isotherms for a well have been calculated, extrapolating them across a basin is useful. The isotherms are seldom laterally horizontal for very far because of the following three factors:

1. Nonplanar geometry of sediments
2. Movement of fluids
3. Regional variations in heat flow

When strata are folded or where formations are markedly lenticular, anomalies are likely to occur in the geometry of isotherms. Two local variations are of considerable interest. Table 4.3 shows that salt has a far higher conductivity than most sediments (in the order of 5.5 W/m °C).

Evans (1977), in a study of North Sea geothermal gradients, noted how isotherms dome up over salt diapirs, and are depressed beneath them, because of the high thermal conductivity of evaporites (Fig. 4.9). This work has been confirmed in studies in other parts of the world. Rashid and McAlary (1977) and Rashid (1978) studied the thermal maturation of kerogen in two wells on the Grand Banks of Newfoundland. The Adolphus 2K-41 on the crest of a salt structure contained kerogen with a higher degree of maturation than the Adolphus D-50 some 3 km down flank. Conversely, sandstones lose their porosity in response to many variables, but heat is one of most important. Thus sandstones may be more cemented above a salt dome than are adjacent sands at comparable depths. Figure 4.10 shows that isotherms are depressed beneath a salt dome. Thus sandstones may have higher porosities than their lateral equivalents, and source rocks may be less mature than their lateral equivalents. This phenomenon has been noted in the presalt plays of the Gulf of Mexico, Brazil, and West Africa (Mello et al., 1995).

In contrast to salt, mud diapirs of highly porous overpressured clay have an anomalously low thermal conductivity. The isotherms within the clay will be closely spaced and depressed over the dome. Extensive overpressured clay formations act as an insulating blanket, trapping thermal energy and aiding source rock maturation.

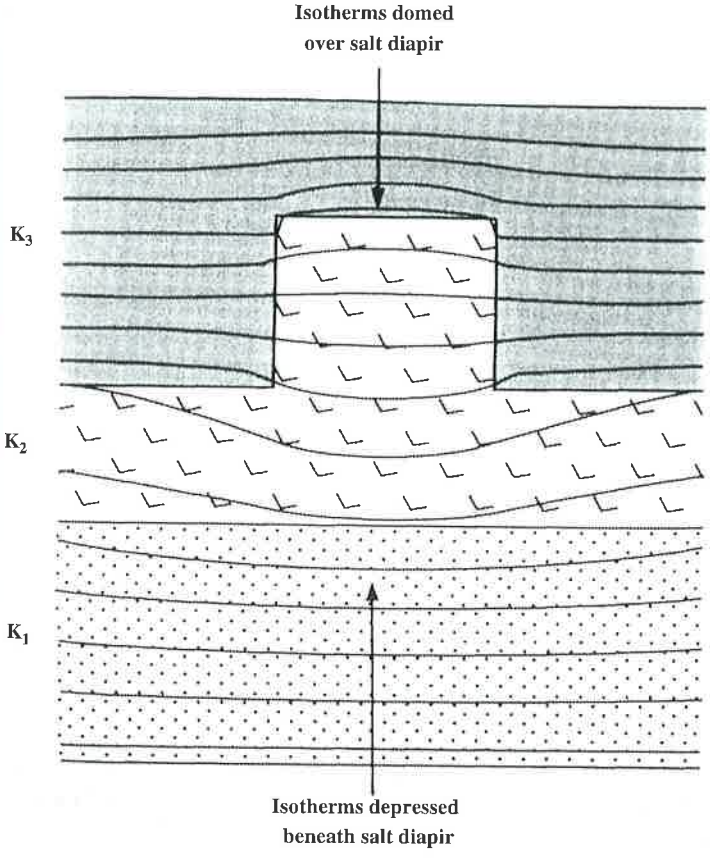

FIGURE 4.10 Isotherms modeled for a salt dome. Contours at 20 °C. Conductivities are as follows: postsalt sediments, $K_3 = 1.74$ W/m °C; Zechstein (Permian) salt, $K_2 = 4.22$ W/m °C; pre-Permian Carboniferous clastics, $K_1 = 2.82$ W/m °C. Note how source rocks will be abnormally mature above a salt dome and abnormally immature beneath one. Conversely, reservoir sands may be abnormally cemented above and abnormally porous beneath a diapir. *Developed from Evans (1977).*

Igneous intrusions are a further cause of local perturbations in heat flow, since they may cause positive heat flow anomalies long after the magma was emplaced (Sams and Thomas-Berts, 1988). The resultant thermal chimney may result in the development of a convection cell that draws connate water into the flanks of the intrusion and expels it from the crest. This mechanism may be responsible for the emplacement of the petroleum that is found in fractured reservoirs in many granites. It has been invoked, for example, to explain the petroleum reservoirs in fractured basement of offshore Vietnam (Schnip, 1992; Dmitriyevsky, 1993) and in the granites of southwest England (Selley, 1992).

A further cause of local perturbations in heat flow results when waters are rapidly discharged along open faults. This phenomenon has been described for some of the Viking Graben boundary faults of the North Sea (Cooper et al., 1975) and from growth faults of the Gulf Coast (Jones and Wallace, 1974).

4.2.3 Regional Thermal Variations

The heat flow of the earth's crust has previously been defined as the product of the geothermal gradient and the thermal conductivity. Data on global heat flow and discussions of its regional variation have been given by Lee (1965) and Sass (1971). The global average heat flow rate is of the order of 1.5 $\mu cal/cm^2$ s. Abnormally high heat flow occurs along midocean ridges and intracratonic rifts, where magma is rising to the surface and the crust is thinning and separating. Conversely, heat flow is abnormally low at convergent plate boundaries, where relatively cool sediments are being subducted into the mantle (Klemme, 1975).

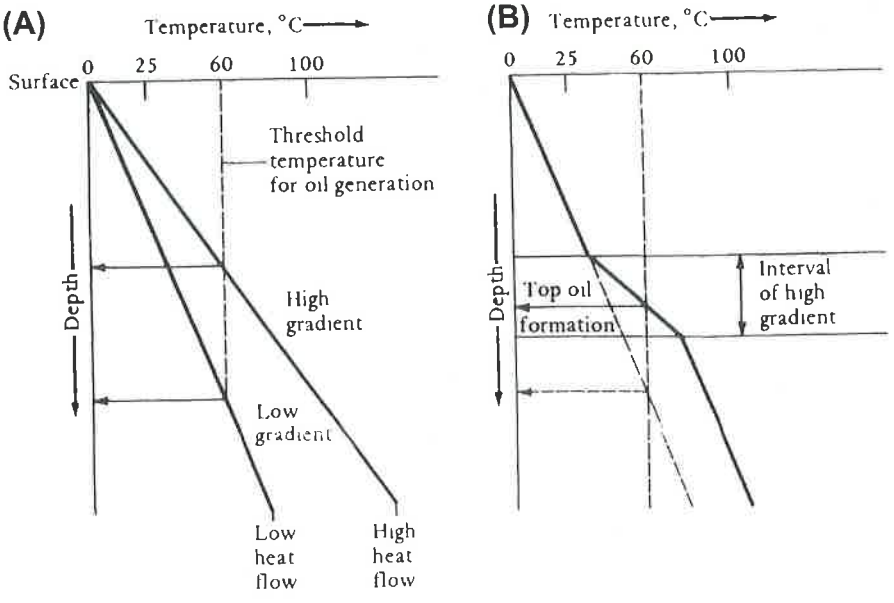

FIGURE 4.11 (A) Depth–temperature graph showing how the top of the oil generation zone rises with increasing geothermal gradient. (B) Depth–temperature graph showing how a formation with a low conductivity and high gradient raises the threshold depth of oil generation.

Regional variations in heat flow affect petroleum generation, as discussed in the next chapter. Data showing that oil generation occurs between temperatures of 60 and 120 °C will be presented. In areas of high heat flow, and hence high geothermal gradient, the optimum temperature will be reached at shallower depths than in areas of low heat flow and geothermal gradient (Fig. 4.11(A)). Note also the effect of low conductive formations. With their high geothermal gradients they raise the depth at which the oil window is entered (Fig. 4.11(B)). Thus oil generation begins at greater depths in subductive troughs than in rift basins. Layers of low-conductivity rock may raise the depth at which oil generation begins.

4.3 SUBSURFACE PRESSURES

4.3.1 Measurement

Subsurface pressures can be measured in many ways. Some methods indicate pressure before a well is drilled, some operate during drilling, and others operate after drilling.

In wildcat areas with minimal well control the interval velocities calculated from seismic data may give a clue to pressure, or at least overpressure. Velocity generally increases with depth as sediments compact. A reversal of this trend may indicate undercompacted and hence overpressured shales (Fig. 4.12).

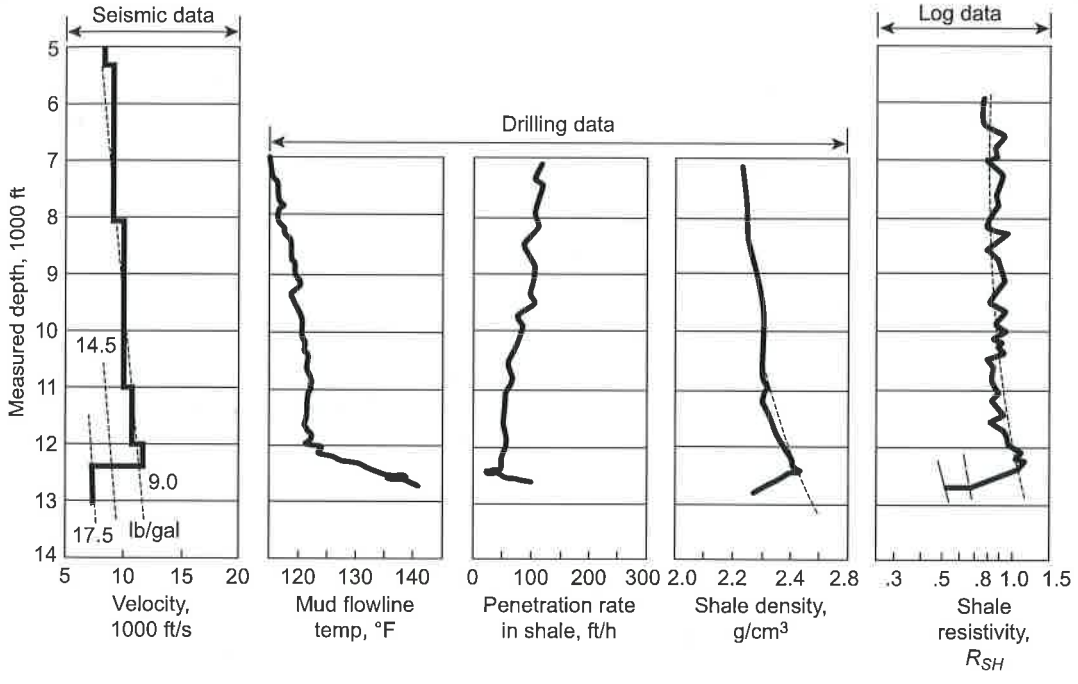

FIGURE 4.12 Various indicators of overpressure detection. In this well a zone of overpressure is present below 12,400 ft. *After Fertl and Chilingarian (1976) © SPE-AIME.*

While a well is being drilled, a number of parameters may indicate abnormal pressure. These parameters include a rapid increase in the rate of penetration, a rapid increase in the temperature of the drilling mud, and a decrease in the density of shale cuttings. A particularly useful method is the drilling (d) exponent (Jordan and Shirley, 1966). This method takes into account that the rate of penetration of the bit reflects not only the degree of compaction of the sediments but also the weight on the bit and the rotary speed:

$$d \text{ exponent} = \frac{\log(R/60N)}{\log(12W/106D)},$$

where

R = rate of penetration (ft/h)
N = rotary speed (rpm)
W = weight on bit (lb)
D = diameter of borehole (in.)

The d exponent is plotted against depth as the well is drilled. It will decrease linearly until reaching the top of abnormal pressure, at which depth it will increase.

When these methods suggest that a zone of overpressure has been penetrated, it may be wise to stop drilling and run logs. Sonic, density, and neutron logs may all show a sudden increase in porosity, whereas resistivity may sharply decrease (Hottman and Johnson, 1965). Since logs respond to more than one variable, no single log is diagnostic. Lithological changes may give similar responses.

The problem with all these methods of detecting overpressure is the difficulty of establishing at what point deviation from the normal is sufficiently clear for overpressure to be proven. By that time it may be too late, because the well may have kicked. The reversed spontaneous potential (SP) curve, mentioned in Chapter 3, is another method of identifying overpressure ahead of the drill bit.

Once a well has been safely drilled, pressure can be measured by several methods. A pressure bomb, in which pressure is recorded against time, can be lowered into the hole. The drill stem test, in which the well is allowed to flow for several short periods while the pressure is monitored, is another method of measuring pressure. Drill stem tests may give good measurement results not only of the pressure but also of the flow rate (and hence permeability) of the formation. Fluids may also be allowed to flow to the surface for collection and analysis. For further details, see Bradley (1975) and Dickey (1979). Some wireline tools are designed to measure formation pressures and recover fluids from zones of interest. Sometimes they work.

4.3.2 Basic Principles

Pressure is the force per unit area acting on a surface. It is generally measured in kilograms per square centimeter (kg/cm^2) or pounds per square inch (psi). The several types of subsurface pressure can be classified as follows:

- Overburden pressure
  - 1. Lithostatic
  - 2. Fluid pressure
    - (a) Hydrostatic
    - (b) Hydrodynamic

The lithostatic pressure is caused by the pressure of rock, which is transmitted through the subsurface by grain-to-grain contacts. The lithostatic pressure gradient varies according to depth, the density of the overburden, and the extent to which grain-to-grain contacts may be supported by water pressure. It often averages about 1 psi/ft.

The fluid pressure is caused by the fluids within the pore spaces. According to Terzaghi's law (Terzaghi, 1936; Hubbert and Rubey, 1959).

$$s = p + o,$$

where s = overburden pressure, p = lithostatic pressure, and o = fluid pressure. As fluid pressure increases in a given situation, the forces acting at sediment–grain contacts diminish and lithostatic pressure decreases. In extreme cases this effect may transform the sediment into an unstable plastic state.

In the oil industry fluid pressure is generally calculated as follows:

$$p = 0.052 \times wt \times D,$$

where p = hydrostatic pressure (psi), wt = mud weight (lb/gal), and D = depth (ft).

The two types of fluid pressure are hydrostatic and hydrodynamic. The hydrostatic pressure is imposed by a column of fluid at rest. For a column of fresh water (density 1.0) the hydrostatic gradient is 0.433 psi/ft, or 0.173 kg/cm^2 m. For water with 55,000 ppm of dissolved salts the gradient is 0.45 psi/ft; for 88,000 ppm of dissolved salts the gradient is about 0.465 psi/ft. These values are, of course, temperature dependent. Figure 4.13 shows the relationship between lithostatic and hydrostatic pressure.

The second type of fluid gradient is the hydrodynamic pressure gradient, or fluid potential gradient, which is caused by fluid flow. When a well is drilled, pore fluid has a natural tendency to flow into the well bore. Normally, this flow is inhibited by the density of the drilling mud. Nonetheless, the ability to measure the level to which the fluid would rise if the well were open is important. This level is termed the *potentiometric* or *piezometric* level and is calculated as follows:

$$\text{Elevation to potentiometric level} = \frac{P}{W} - (D - E),$$

where

P = bottom hole pressure (psi)
W = weight of fluid (psi/ft)
D = depth (ft)
E = elevation of kelly bushing above sea level (ft)

The potentiometric level of adjacent wells may be contoured to define the potentiometric surface. If this surface is horizontal, then no fluid flows across the region and the fluid pressure is purely hydrostatic. If the potentiometric surface is tilted, then fluid is moving across the basin in the direction of dip of the surface and the fluid pressure is caused by both hydrostatic and hydrodynamic forces (Fig. 4.14). Formation water salinity commonly increases in the direction of dip of the potentiometric surface (Fig. 4.15). Where the pressure gradient is hydrostatic (approximately 0.43 psi/ft), the pressure is termed normal. Abnormal gradients

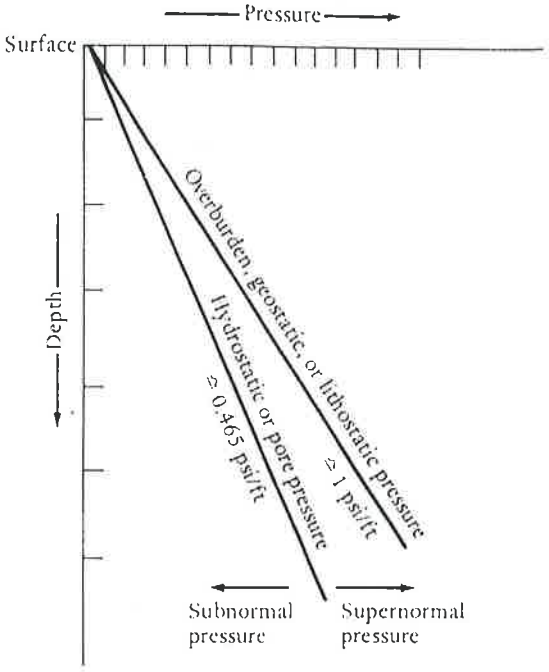

FIGURE 4.13 Depth–pressure graph illustrating hydrostatic and lithostatic (geostatic) pressures and concepts.

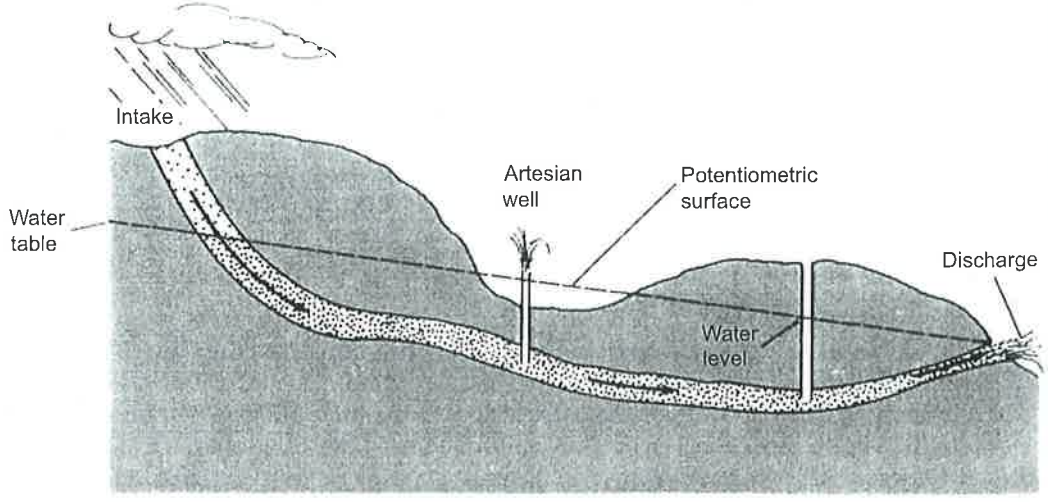

FIGURE 4.14 Sketch illustrating the concept of the potentiometric, or piezometric, surface.

may be subnormal (less than hydrostatic) or supernormal (above hydrostatic). The level to which formation fluid would rise or fall to attain the potentiometric surface is expressed as the fluid potential. Hubbert (1953) showed that this potential could be calculated as follows:

$$\text{Fluid potential} = Gz + \frac{P}{\rho},$$

where

G = the acceleration due to gravity
z = datum elevation at the site of pressure measurement
P = static fluid pressure
ρ = density of the fluid

The fluid potential is also directly related to the head of water, h:

$$\text{Fluid potential} = hG.$$

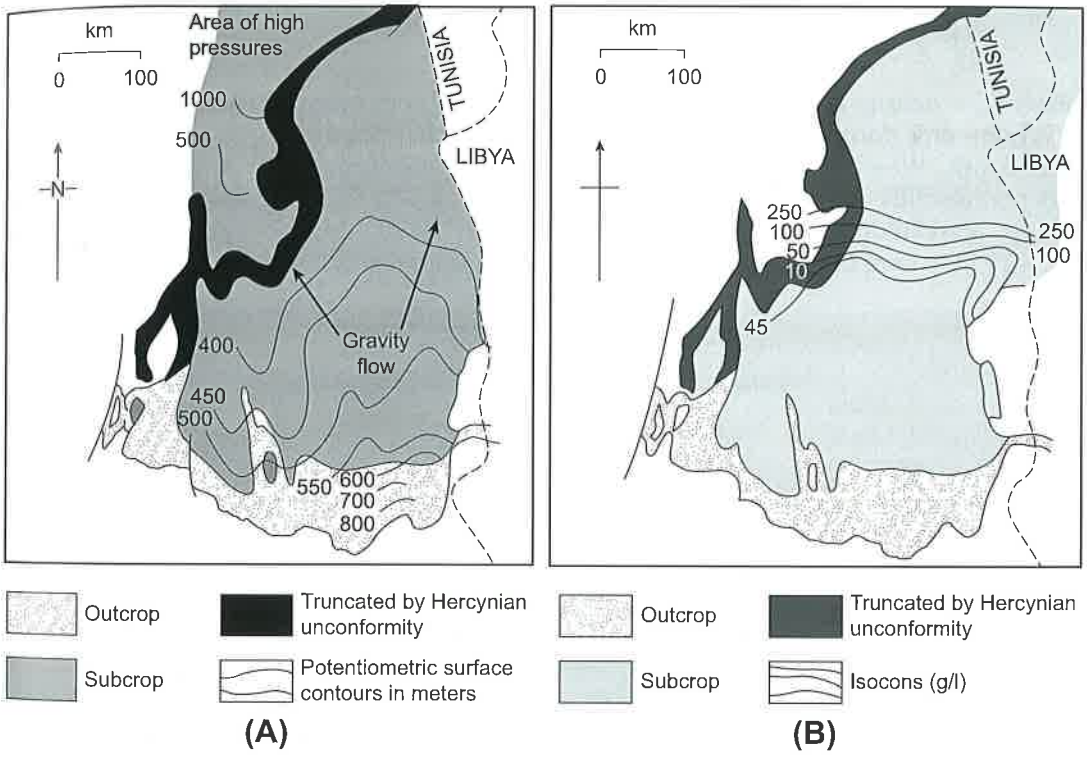

FIGURE 4.15 (A) Potentiometric and (B) isocon maps of the Silurian–Lower Devonian (Acacus and Tadrart) reservoir sandstones of eastern Algeria. Note how the potentiometric surface drops northward with increasing formation water salinity. *Modified from Chiarelli (1978); reprinted by permission of the American Association of Petroleum Geologists.*

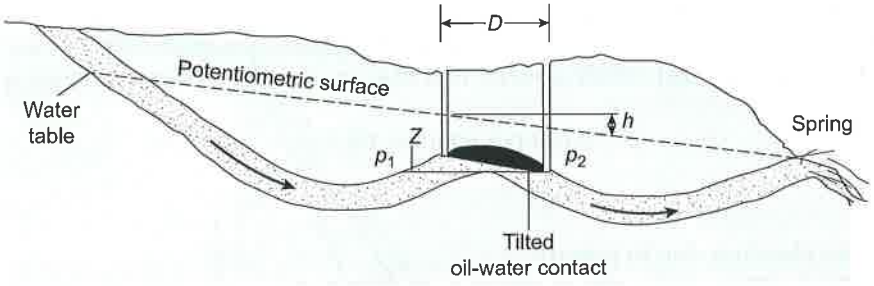

FIGURE 4.16 Sketch showing how the slope of an oil–water contact may be due to hydrodynamic flow.

Sometimes oil/water contacts are not horizontal, but tilted. Hydrodynamic flow is one of several causes of such contacts. Hubbert (1953) showed how in such cases the slope of the contact is related to the fluid potential (Fig. 4.16):

$$\frac{z}{d} = \frac{h}{d}\frac{(\rho_w)}{\rho_w - \rho_o},$$

where ρ_w = density of water, ρ_o = density of oil, and d = distance between wells.

Within any formation with an open-pore system, pressure will increase linearly with depth. When separate pressure gradients are encountered in a well, it indicates that permeability barriers separate formations (Fig. 4.17). This principle can be a useful aid to correlating reservoir formations between wells. In the situation shown in Fig. 4.18, it is tempting to assume that the upper, middle, and lower sands are continuous

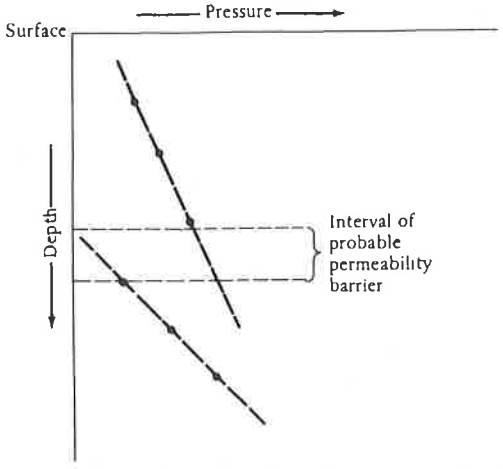

FIGURE 4.17 Pressure–depth plot of a well showing different gradients. These gradients suggest the existence of a permeability barrier between the two intervals with uniform, but different, gradients.

from well to well. Pressure gradient plots may actually reveal a quite different correlation. This difference is particularly common in stacked regressive barrier bar sands. Borehole pressure data are also used to construct regional potentiometric maps, which may be used to locate hydrodynamic traps.

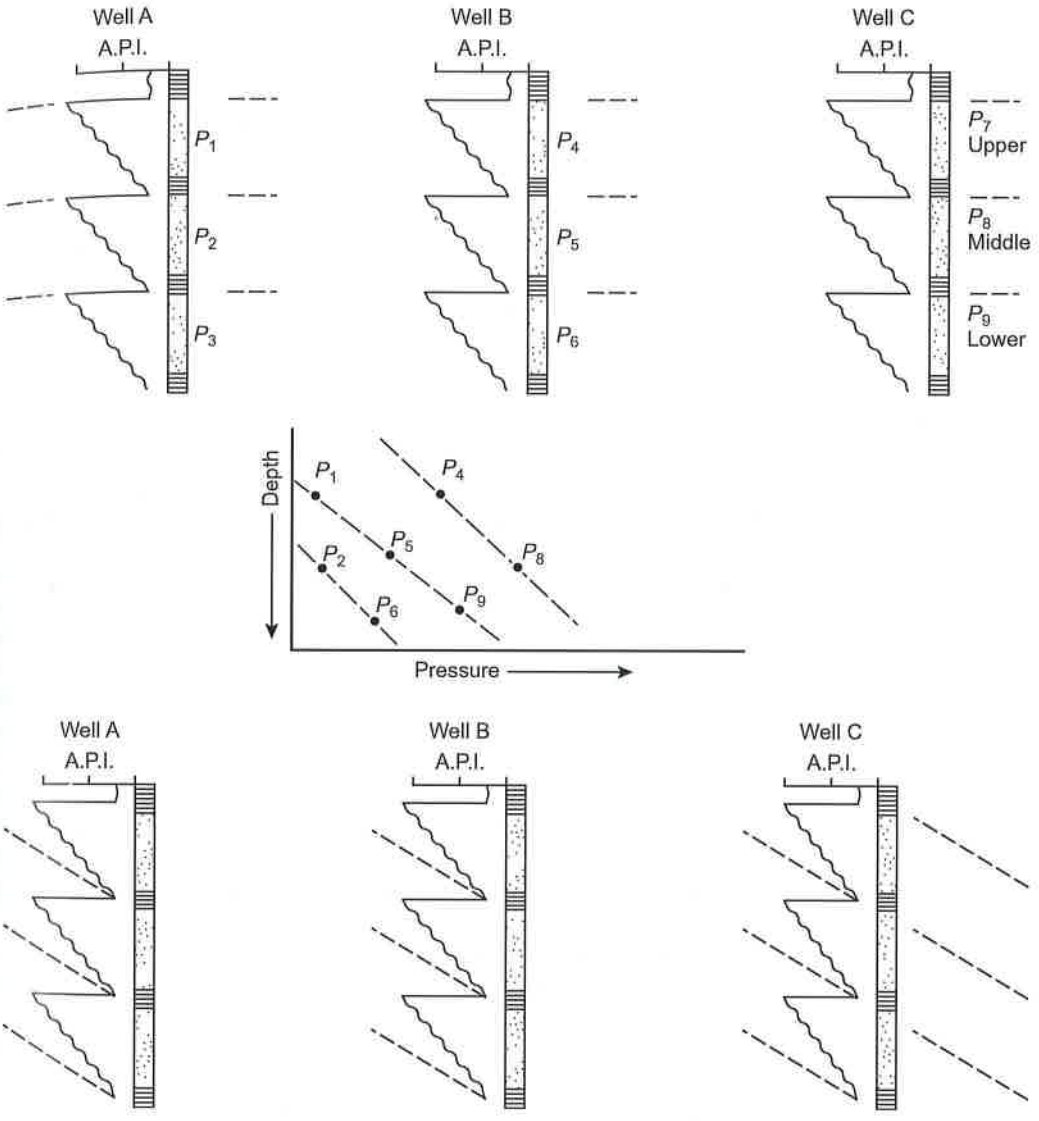

FIGURE 4.18 Sketches showing how the obvious correlation of multistorey sands (top) may be shown to be incorrect from pressure data (center). The bottom correlation is common in laterally stacked barrier bar sands.

4.3.3 Supernormal Pressure

Supernormal pressures are those pressures that are greater than hydrostatic. They are found in sediments ranging in age from Cambrian to recent, but are especially common in Tertiary deltaic deposits, such as in the North Sea, Niger Delta, and Gulf Coast of Texas. Study of the causes and distribution of overpressuring is very important because overpressuring presents a hazard to drilling and is closely related to the genesis and distribution of petroleum. Overpressuring occurs in closed-pore fluid environments, where fluid pressure cannot be transmitted through permeable beds to the surface. Thus the two aspects to consider are the nature of the fluid barrier and the reason for the pressure buildup (Jacquin and Poulet, 1973; Bradley, 1975; Barker, 1979; Plumley, 1980; Luo et al., 1994).

The permeability barrier, which inhibits pressure release, may be lithological or structural. Common lithological barriers are evaporites and shales. Less common are the impermeable carbonates or sandstones, which may also act as seals. Structural permeability barriers may be provided by faults, although as discussed in detail later, some faults seal and others do not.

Fertl and Chilingarian (1976) have listed 13 possible causes of overpressure. Only the more important causes are discussed here:

1. Artesian
2. Structural
3. Compactional
4. Diagenetic

The concept of the potentiometric surface and artesian pressure has just been dealt with. In cases such as the Silurian–Devonian sandstones of Algeria (Fig. 4.15) the potentiometric surface at the edge of the basin drops toward the center. In the central part of the basin, however, the surface rises, so very high pressures occur where the sandstones are sealed beneath the Hercynian unconformity.

Structural deformation can cause overpressure in several ways. At the simplest level a block of sediment can be raised between two sealing faults and, if fluids have no other egress, the pore pressure will be unable to adjust to the new lower hydrostatic pressure. In more complex settings compression of strata during folding can cause overpressure if excess fluid has no means of escape. This situation is most likely to happen when permeable strata are interbedded with evaporites, as in Iran. The evaporites can be involved in intense compression, deforming plastically and preventing excess fluid from bleeding off through fractures or faults.

The third and perhaps most common type of overpressure is caused by compaction, or rather the lack of it. This situation is especially common in muddy deltas where deposition is too fast for sediments to compact and dewater in the normal way. This topic has been studied in great detail (see, for example, Athy (1930), Jones (1969), Perry and Hower (1970), Rieke and Chilingarian (1973), Fertl (1977)).

Figure 4.19 presents the basic effects of compaction on overpressure. On a delta plain sands and clays are commonly interbedded. The sands are permeable and communicate with the surface. As the delta plain sediments are buried, the clays compact, lose porosity, and increase in density. Excess pore fluids move into the sands and escape

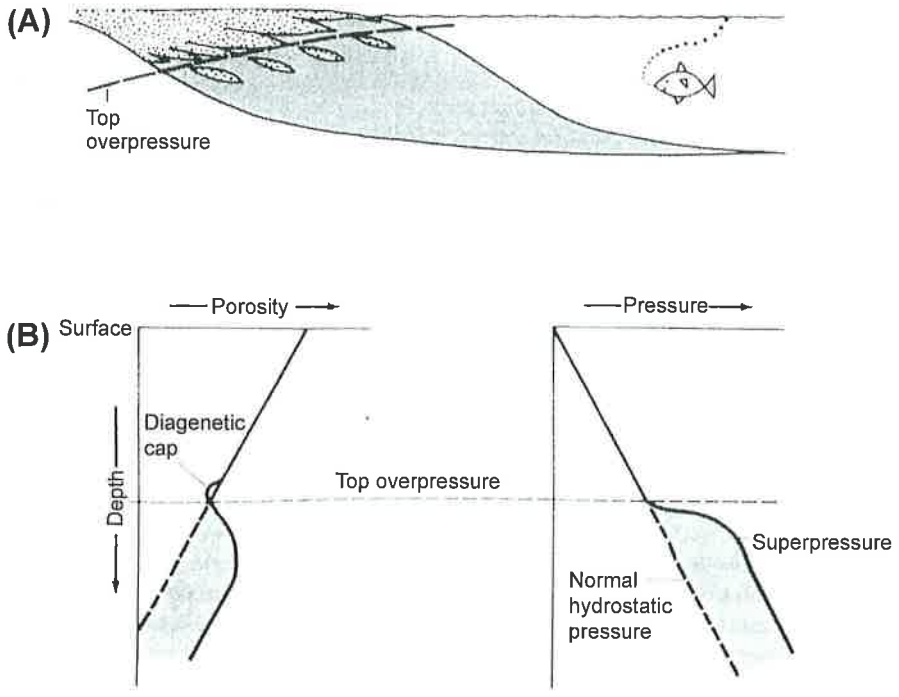

FIGURE 4.19 (A) Cross-section through a delta to show that overpressuring occurs beneath the break-up zone where there are no longer any sand beds to act as conduits to permit muds to dewater. (B) depth–porosity and depth–pressure curves, indicating how overpressuring may occur due to undercompaction.

to the surface. Thus although pore pressure increases with burial, it remains at the hydrostatic level. On the seaward side of the delta, however, sands become discontinuous and finally die out. As the delta progrades basinward, the delta plain sediments overlie the prodelta muds. The overburden pressure increases on the prodelta muds, but, lacking permeable conduits, they cannot dewater. Porosity remains high, and pore pressure exceeds hydrostatic. This type of overpressure has several important implications for petroleum geology. First, overpressured shales are a drilling hazard. Methods of predicting overpressure ahead of the drill bit were discussed in Chapter 3. Secondly, overpressured shales have lower densities and lower thermal conductivities than normally pressured shales.

The lower density of overpressured shales compared with normally compacted sediments means that they tend to flow upward and be replaced by denser, normally compacted sediments from above. This flow causes growth faults and clay diapirs, which can form important hydrocarbon traps, as discussed and illustrated later. The significance of the low thermal conductivity of overpressured shales was noted earlier. By increasing the geothermal gradient, oil generation can occur at shallower depths.

There is now a growing body of evidence that the dewatering of overpressured shale is a catastrophic and episodic process (Capuano, 1993). For example, 3D seismic studies of the

Tertiary sediments of the North Sea basin reveal the existence of alternations of zones with continuous reflectors, and intervals with polygonal fault systems (Cartwright, 1994). It is argued that the continuous zones are condensed stratigraphic sequences whose slow sedimentation rates lead to relatively low porosities. These zones behave as regional seals. The intervening intervals were deposited more rapidly, with higher original porosities, and became overpressured during burial. Their polygonal fault systems suggest that these zones underwent catastrophic expulsion of excess pore fluids (Fig. 4.20). Roberts and Nunn (1995) present data to show that the rapid expulsion of hot overpressured fluids raises temperatures in the overlying sediment cover by up to 20 °C. They argue that basins throb at periodicities of 10,000–500,000 years. The concept that overpressure is not bled off in a slow and steady manner, but by episodic hot flushes, has important implications for petroleum migration and for sandstone diagenesis. We return to this topic and discuss it at greater length in Chapters 5 and 6.

A fourth cause of overpressure is mineralogical reactions during diagenesis. A number of such reactions have been noted, including the dehydration of gypsum to anhydrite and water, and the alteration of volcanic ash to clays and carbon dioxide. Probably the most important reactions responsible for overpressure are those involving clays. In particular the dewatering of montmorillonitic clays may be significant. As montmorillonitic clays are compacted, they give off not only free-pore water but also water of crystallization. The temperatures and pressures at which these reactions occur are similar to those at which oil generation occurs. This phenomenon may be closely linked to the problem of the primary migration of oil, as discussed in the next chapter. Other diagenetic reactions occur in shales, which may not only increase pore pressure but also decrease permeability. In particular, a cap of carbonate-cemented shale often occurs immediately above an overpressured interval.

Finally, overpressuring can be caused during production either by fluid injection schemes or by faulty cementing jobs in which fluids move from an overpressured formation to a normally pressured one. In some presently normally pressured basins the presence of fibrous calcite along veins and fractures may be a relict indicator of past overpressures (Stoneley, 1983).

4.3.4 Subnormal Pressure

Subnormal pressures are those pressures that are less than the hydrostatic pressure. Examples and causes of subnormal pressures have been given by Fertl and Chilingarian (1976), Dickey and Cox (1977), and Bachu and Underschultz (1995).

Subnormal pressures will only occur in a reservoir that is separated from circulating groundwater by a permeability barrier; were this not so, the reservoir would fill with water and rise to hydrostatic pressure (Fig. 4.21). Subnormal pressures can be brought about by producing fluids from reservoirs, especially where they lack a water drive.

Naturally occurring subnormal pressures are found around the world in both structural and stratigraphic traps. Fertl and Chilingarian (1976) cite pre-Pennsylvanian gas fields of the Appalachians and the Morrow sands of trap in northwestern Oklahoma. Dickey and Cox (1977) cite subnormal pressures in the Cretaceous barrier bars from the Viking sands of Canada to the Gallup Sandstone of New Mexico.

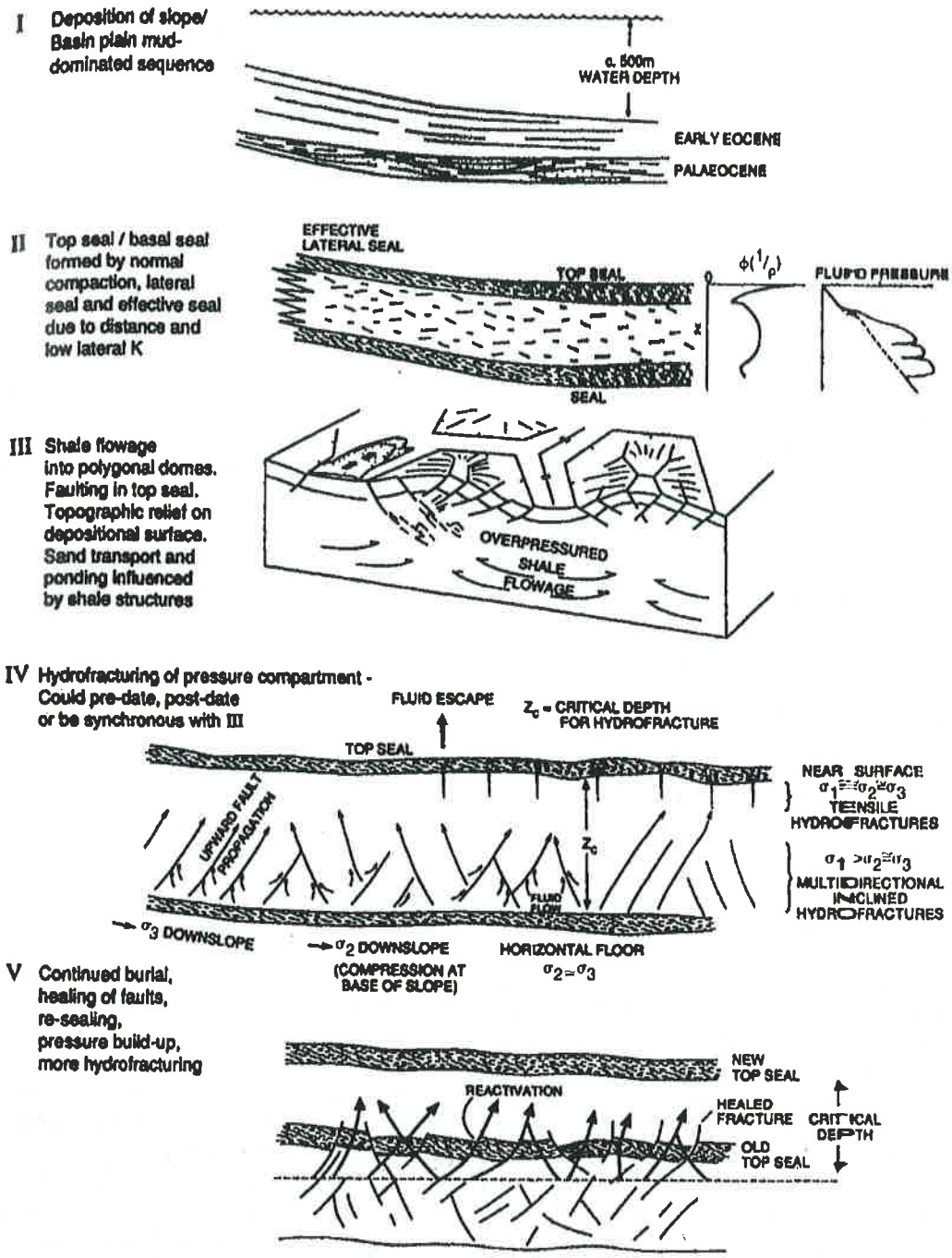

FIGURE 4.20 Geophantasmograms to explain how polygonal fault systems in the Tertiary section of the North Sea Basin may indicate the episodic expulsion of overpressured fluids. This mechanism has important implications for petroleum migration and for sandstone diagenesis. *Reprinted from Marine and Petroleum Geology, vol. II, Cartwright, pp. 587–607. Copyright 1994, with kind permission from Elsevier Science Ltd.*

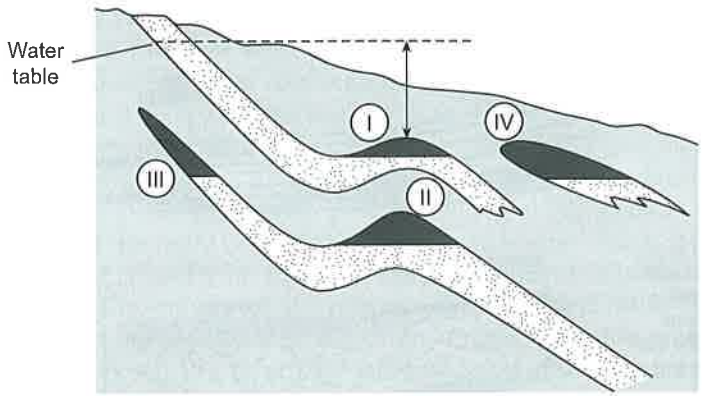

FIGURE 4.21 Cross-section to illustrate the setting of a subnormally pressured trap. Trap I is in fluid communication with the surface and will be normally (hydrostatically) pressured. Traps II and III are in fluid communication with connate waters in the center of the basin. They may be normal or overpressured. Trap IV, however, is completely enclosed in impermeable shale. Virgin pressure may be sub- or supernormal, but will drop to subnormal during production because there is no aquifer to maintain reservoir pressure. *After Dickey and Cox (1977), reprinted by permission of the American Association of Petroleum Geologists.*

Subnormal pressures may be caused by three main processes:

1. Increase in pore volume
   a. by decompression
   b. by fracturing
2. Decrease in reservoir temperature
3. The production of petroleum from a sealed reservoir

In a confined system an increase of pore volume will cause pressure to drop as the fluids expand to fill the extra space. Pore volume may be expanded by decompression or tectonism. Erosion of rock above a normally pressured reservoir will cause a decrease in overburden pressure and hence an expansion of the reservoir rock, accompanied by a pro rata increase in pore volume and a drop in fluid pressure. Underpressuring attributed to pore-space rebound in response to isostatic uplift and erosion of the cover occurs in the deeper part of the Llanos Basin of Columbia adjacent to the Cordilleran mountain front. Here regional aquitards separate underpressured sediments of the basin nadir from shallower normally pressured sediments (Villagas et al., 1994). A similar pattern of water flow and underpressuring has been reported from the southwestern Alberta Basin of Canada (Bachu and Underschultz, 1995). Again, at shallow depths, groundwater flows eastward, largely in response to the hydrodynamic head generated in the Rocky Mountains. Beneath regional aquitards, however, water flows westward to become underpressured adjacent to the mountain front, where it has been estimated that there has been up to 4 km of post-Cretaceous erosion and uplift (Fig. 4.22).

A second way in which pore volume may increase is when extensional fractures form over the crest of an anticline. This mechanism has been invoked to explain the subnormal pressure of the Kimmeridge Bay field of Dorset (Brunstrom, 1963).

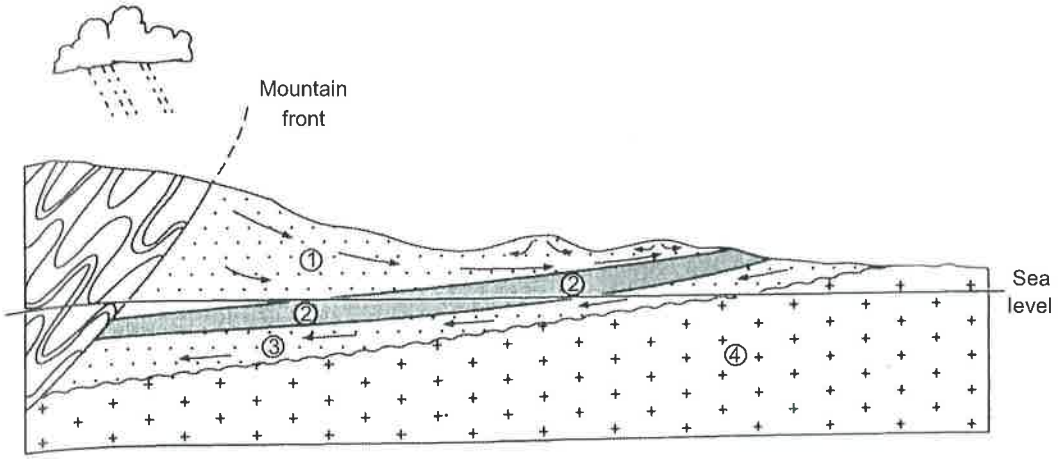

FIGURE 4.22 Cross-section through a back arc basin to show hydrologic regimes and water flow directions (per arrows). Based on the Alberta Basin of Canada and the Llanos Basin of Columbia (see Bachu and Underschultz (1995), and Villagas et al. (1994); respectively.) (1) Shallow zone where flow is driven across the basin away from the hydrodynamic head generated by the mountain range. Petroleum may be trapped in hydrostatic or hydrodynamic traps. (2) Zone of potential aquitards that may separate shallow from deep hydrological regimes. (3) Deep zone where water flows from the basin edge toward the mountain front. Underpressured reservoirs may occur adjacent to the mountain front due to isostatic uplift, erosion, and pore-space rebound. (4) Impermeable basement.

The second main cause of subnormal pressure is a decrease in geothermal gradient, which will cause reservoir fluids to cool and shrink, and thus decrease in pressure.

Finally, underpressure may develop where a petroleum reservoir occurs completely enclosed in impermeable formations, such as a reef enclosed by evaporites, or a channel or shoestring sand enclosed by shales. In these situations virgin pressure may be at or above hydrostatic. As the reservoir is produced, however, there will be no aquifer to allow water to flow in to replace the produced petroleum. Thus the time may come when the pressure in the reservoir drops below hydrostatic.

4.3.5 Pressure Compartments

Many sedimentary basins contain a layered arrangement of two superimposed hydrogeological systems. The shallow system extends down to a depth of approximately 3000 m or subsurface temperatures of 90 to 100 °C. Pore waters freely migrate in the shallow system.

The deeper seal-bounded fluid pressure system or compartments is where much of the world's oil and gas has been generated (Hunt, 1990). The seal for the compartments appears to be caused by carbonate mineralization along a thermocline (90 to 100 °C). The deep compartments are not basinwide and are generally overpressured due to generation of oil and gas and thermal expansion of pore fluids. This seal-bounded compartment is a restricted flow system. Some compartments that are underpressured may be caused by thermal contraction of confined fluids as buried rocks cool during continued uplift or erosion at

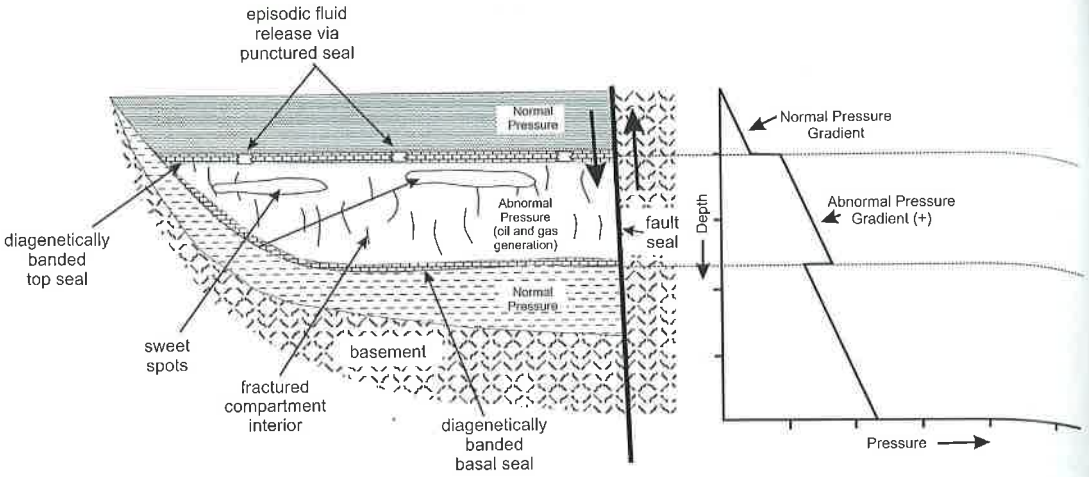

FIGURE 4.23 Diagrammatic basin-scale pressure compartment defined by diagenetically banded transbasinal top seal, stratum-localized bottom seal, fault side seal, and a fractured interior (*modified from Ortoleva, 1994*). Pressure–depth plot illustrates abnormal pressure compartment.

the surface. Compartments have great longevity and they can undergo changes from overpressure to normal pressure to underpressure as basins go through stages of sinking and deposition, to quiescence, to basin uplift and erosion. The fluid pressure compartment has the unique characteristic of exhibiting internal dilation fractures.

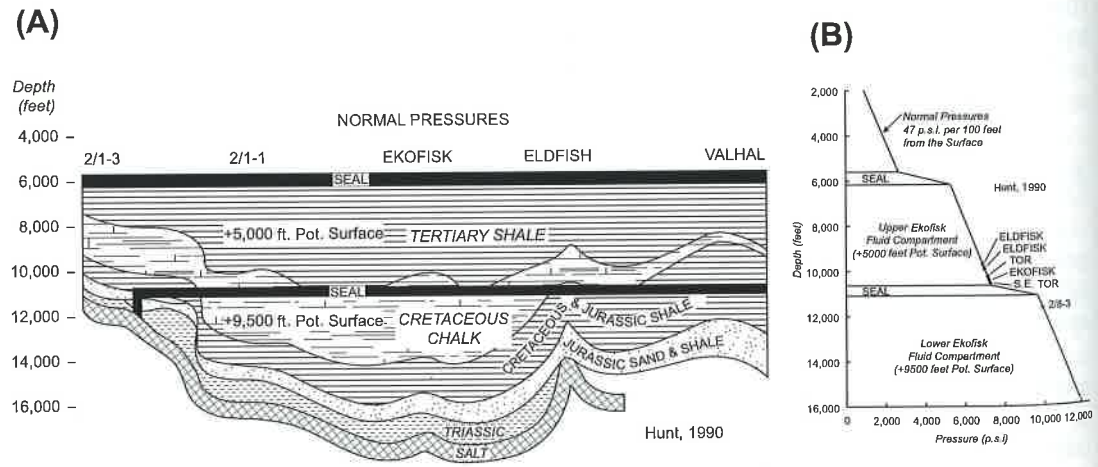

FIGURE 4.24 (A) Approximate position of seals of upper and lower Ekofisk pressure compartments in southern Central Graben, North Sea Basin (Hunt, 1990). (B) Pressure–depth plot for Ekofisk and nearby fields in Central Graben, North Sea Basin (Hunt, 1990).

The generation of oil and gas within compartments plus thermal expansion of pore fluids eventually causes fracturing at the top of the compartment seal. Oil and gas can migrate into structural and stratigraphic traps in the shallow normally pressured regime. Compartments are thought to reseal and pressure can build up again and the process will repeat itself.

Some basins have a third system or compartment that is normally pressured (Fig. 4.23).

Figure 4.24 illustrates pressure compartments in the southern Central Graben, North Sea basin. Beneath each seal the pressure gradient increases.

4.4 SUBSURFACE FLUID DYNAMICS

4.4.1 Pressure–Temperature Relationships

Temperature and pressure in the subsurface have been reviewed separately; they are now examined together. More detailed accounts will be found in petroleum reservoir engineering textbooks, such as Archer and Wall (1986). From the laws of Boyle and Charles, the following relationship exists:

$$\frac{\text{Pressure} \times \text{volume}}{\text{Temperature}} = \text{a constant.}$$

This basic relationship governs the behavior of fluids in the subsurface, as elsewhere, and is particularly important in establishing the formation volume factor in a reservoir. For a given fluid at a constant pressure there is a particular temperature at which gas bubbles come out of liquid and at which they condense as temperature decreases. Similarly, at a uniform temperature there is a particular pressure at which liquid evaporates as pressure drops and gas condenses as pressure increases.

A pure fluid may exist in either the liquid or gaseous state, depending on the pressure and temperature (Fig. 4.25). Above the critical point (*c*), however, only one phase can exist. Subsurface fluids are mixtures of many compounds: connate water contains traces of hydrocarbons in solution; petroleum is a mixture of many different hydrocarbons in liquid and/or gaseous states.

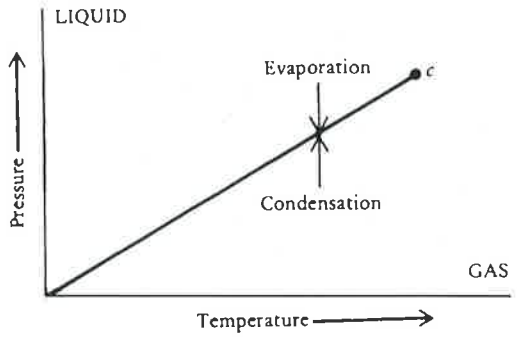

FIGURE 4.25 Pressure–temperature graph for a pure fluid. Above the critical point (*c*) only one phase can exist.

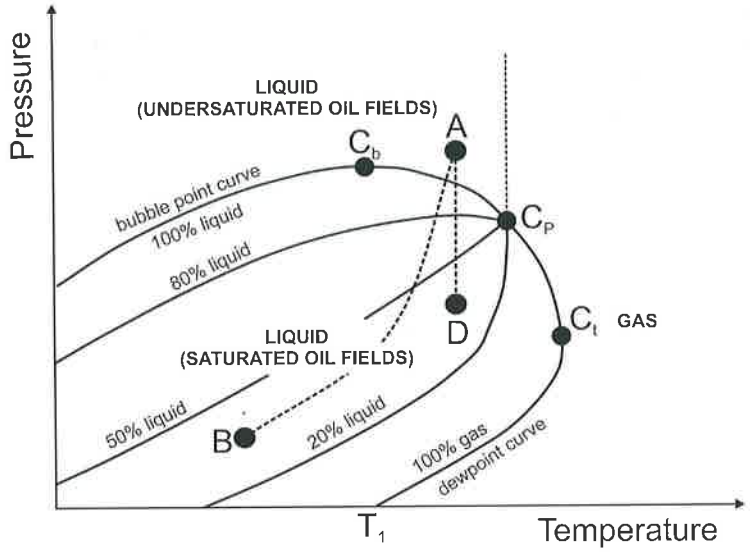

FIGURE 4.26 Pressure–temperature phase diagram of a petroleum mixture. Cb is maximum bubble point called the cricondenbar; Cp is the critical point where bubble point curve and dew point curve coincide; Ct is the cricondentherm, dew point curve maximum temperature value. *(Modified from North (1985).)* A to B symbolizes change from reservoir conditions to near-surface conditions during production; A to D symbolizes pressure drop in a reservoir from production.

A pressure–temperature phase diagram for a petroleum mixture is shown in Fig. 4.26. This figure shows three different fluid phases: liquid, liquid and vapor, and gas. The bubble point line marks the boundary at which gas begins to bubble out of liquid. The dew point line marks the boundary at which gas condenses. These two lines join the critical point (P). Point

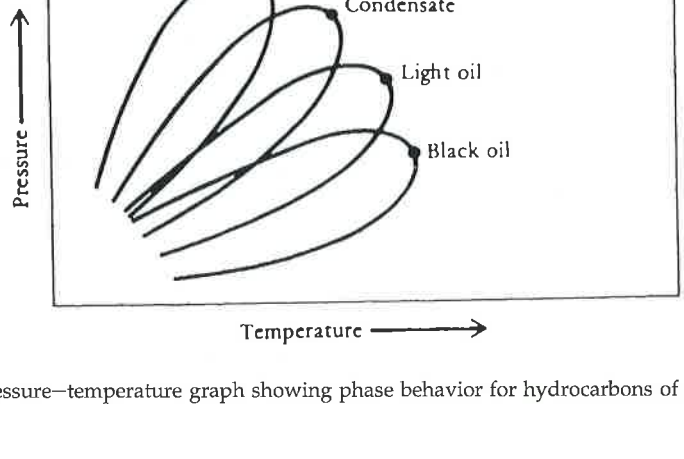

FIGURE 4.27 Pressure–temperature graph showing phase behavior for hydrocarbons of different gravity.

A represents an oil pool with high pressure and moderate temperature. All the gas is in solution. The oil is termed undersaturated. Point B represents the same pool but at lower pressure and the same temperature (production lowers pressure). The pressure is not high enough to keep all the gas in solution in the oil so free gas bubbles come out of the oil and a gas cap may form. This is called the bubble point. Above this point only liquid is present in the reservoir. As pressure continues to drop, the amount of gas released increases and the percentage of liquid oil falls progressively. The oil is termed saturated.

Figure 4.27 shows pressure–temperature curves for various mixtures of hydrocarbons. Several general conclusions can be drawn from these graphs. The amount of gas that can be dissolved in oil increases with pressure and therefore depth. The lower the density (higher the API gravity) of an oil, the more dissolved gas it contains. Within a reservoir with separate oil and gas columns, the two zones are in thermodynamic equilibrium. As production begins and pressure drops, gas will come out of solution and the volume of crude oil will decrease.

4.4.2 Secondary Migration of Petroleum

The effects of pressure and temperature on petroleum are obviously extremely important. They control both the way in which petroleum behaves in a producing reservoir and its migration from source rock to trap. Petroleum production from reservoirs is discussed in Chapter 6. Two types of petroleum migration are recognized.

Primary migration is the movement of hydrocarbons from the source rock into permeable carrier beds (Hunt, 1996). Secondary migration is the movement of hydrocarbons through the carrier beds to the reservoir. Primary migration is still something of a mystery and is reviewed in Chapter 5.

Between leaving the source rocks and filling the pores of a trap, oil must exist as droplets. Therefore, as long as the diameter of the droplets is less than that of the pore throats, buoyancy will move the droplets until they reach a throat whose radius is less than that of the droplet. Further movement can only occur when the displacement pressure of the oil exceeds the capillary pressure of the pore. Capillary pressure is discussed in more detail in Chapter 6, but basically the following relationship exists:

$$\text{Capillary pressure} = \frac{2\,t\cos\theta}{r},$$

where i = interfacial tension between the two fluids, θ = angle of contact, and r = radius of pore. Neither buoyancy nor hydrodynamic pressure alone can exceed the displacement pressure. As the oil droplets build up beneath the narrow throat, however, they increase the pressure at the throat until a droplet is squeezed through the opening. Thus the process will continue until the oil reaches the sediment whose pores are so small that the pressure of the column of oil beneath is insufficient to force further movement. The oil has thus become trapped beneath a cap rock.

The height of the oil column necessary to overcome displacement pressure has been shown by Berg (1975) to be:

$$Z_o = 2\,y\left(\frac{1}{r_t} - \frac{1}{r_p}\right) \Big/ G(\rho_w - \rho_o)$$

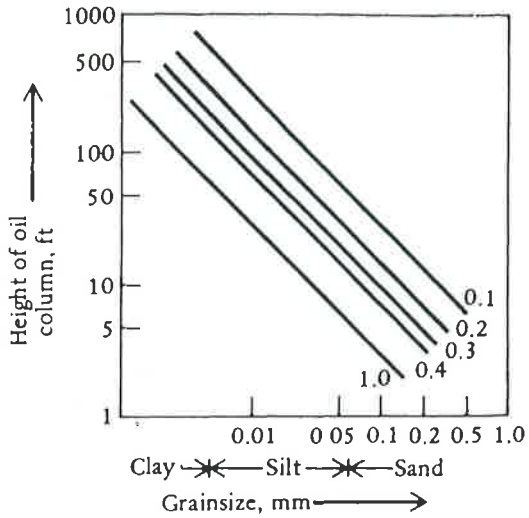

FIGURE 4.28 Graph showing the column of oil trapped by various grades of sediment for oil/water systems of various density differences. Basically, the finer the grain size (i.e., the smaller the pore diameter), the thicker the oil column that it may trap. *Modified from Berg (1975); reprinted by permission of the American Association of Petroleum Geologists.*

where

Z_o = height of oil column
y = interfacial tension between oil and water
r_t = radius of pore throat in the cap rock
r_p = radius of pore throat in the reservoir rock
G = gravitational constant
ρ_w = density of water
ρ_o = density of oil

Figure 4.28 shows the relationship between the height of oil column and grain size for oil–water systems of various density contrasts (a difference of about 0.3 is usual). Oil is

TABLE 4.4 Documented Examples of Long-Distance Lateral Petroleum Migration

Example	Distance km	Distance (mi)	Reference
Phosphoria shale, Wyoming and Idaho	400	(250)	Claypool et al. (1978)
Gulf Coast, USA Pleistocene	160	(100)	Hunt (1996)
Pennsylvanian, northern Oklahoma	120	(75)	Levorsen (1967)
Magellan Basin, Argentina	100	(60)	Zielinski and Bruchhausen (1983)
Athabasca tar sands, Canada	100	(60)	Tissot and Welte (1978)

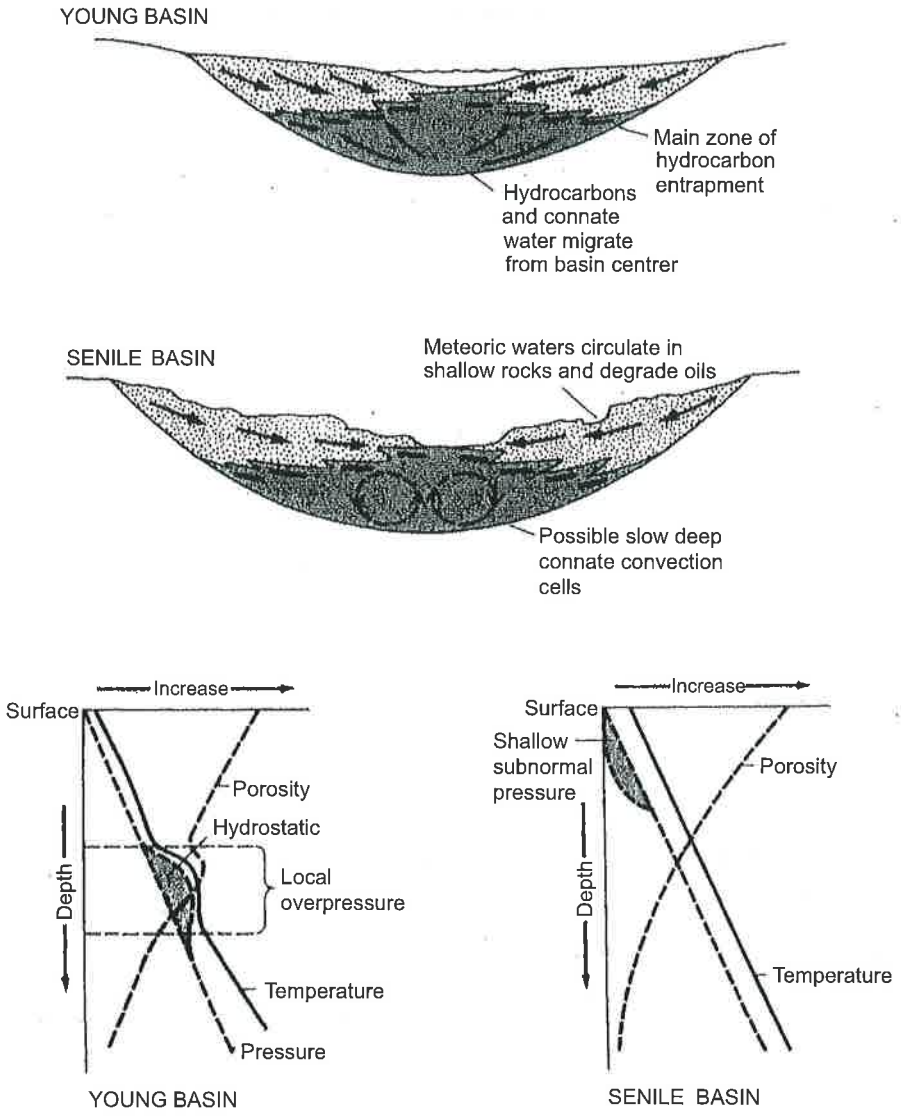

FIGURE 4.29 Cross-sections and depth curves contrasting the fluid dynamics of young and senile sedimentary basins.

thus retained beneath a fine-grained cap rock by capillary pressure in what may be referred to as a *capillary seal*. A capillary seal is likely to be more effective for oil than for the more mobile gases. Gas entrapment may be due not so much to capillary seals but to pressure seals (Magara, 1977). A pressure seal occurs when the pressure due to the buoyancy of the hydrocarbon column is less than the excess pressure of the shales above hydrostatic. Pressure seals are common where overpressured clays overlie normally pressured sands; that is, the

pressure gradient is locally reversed from the usual downward increase to a downward decrease. Examples of this phenomenon are known from many overpressured basins, including the Gulf Coast (Schmidt, 1973). Once oil or gas has reached an impermeable seal, be it capillary or pressure, it will horizontally displace water from the pores.

The lateral distance to which petroleum can migrate has always been debated. Where oil is trapped in sand lenses surrounded by shale, the migration distance must have been short. Where oil occurs in traps with no obvious adjacent source rock, extensive lateral migration must have occurred. Table 4.4 cites some documented examples of long-distance lateral petroleum migration. Note that evidence has been produced for migration of up to 400 km (250 mi).

4.4.3 Fluid Dynamics of Young and Senile Basins: Summary

Familiarity with the subsurface environment, as discussed in this chapter, is necessary in order to understand the generation and migration of oil, to be discussed next. Commonly, rock density, temperature, salinity, and pressure increase with depth, whereas porosity decreases. Local reversals of these trends occur in intervals of overpressure.

Accounts of the dynamics of fluid flow in basins have been given by Cousteau (1975), Neglia (1979), Bonham (1980), Hunt (1990), Powley (1990),, and Parnell (1994). The hydrologic regime of a basin evolves with time from youth to senility. A young basin has a very dynamic fluid system, but deep connate fluid movement declines with age. Immediately after deposition, overburden pressure causes extensive upward movement of water due to compaction. This movement is commonly associated with the migration and entrapment of hydrocarbons. Upward fluid movement may be locally interrupted by zones of overpressure.

As time passes and the basin matures, hydrocarbon generation ceases and overpressure bleeds off to the surface. Pressures become universally hydrostatic or subnormal because of cooling or erosion, isostatic uplift, and reservoir expansion. In some presently normally pressured basins the presence of fibrous calcite along veins and fractures may be a relict indicator of past overpressures (Stoneley, 1983). Meteoric circulation will continue in the shallow surficial sedimentary cover. Deep connate water may continue to move, albeit very slowly, in convection cells. This hypothesis is one explanation for anomalous heat flow data in the southern North Sea. Convection currents are known to exist within petroleum reservoirs (Combarnous and Aziz, 1970). Figure 4.29 summarizes and contrasts the characteristics of young and mature basins.

References

Archer, J.S., Wall, C.G., 1986. Petroleum Engineering Principles and Practice. Graham & Trotman, London.

Athy, L.F., 1930. Density, porosity and compaction of sedimentary rocks. Am. Assoc. Pet. Geol. Bull. 14, 1–24.

Bachu, S., Underschultz, J.R., 1995. Large-scale underpressuring in the Mississippian—Cretaceous succession, southwestern Alberta Basin. AAPG Bull. 79, 989–1004.

Barker, C., 1979. Role of temperature and burial depth in development of sub-normal and abnormal pressures in gas reservoirs. AAPG Bull. 63, 4–14.

Bentor, Y.K., 1969. On the evolution of subsurface brines in Israel. Chem. Geol. 4, 83–110.

Berg, R.R., 1975. Capillary pressures in stratigraphic traps. AAPG Bull. 59, 939–956.

Bonham, L.C., 1980. Migration of hydrocarbons in compacting basins. AAPG Bull. 64, 549–567.

Bradley, J.S., 1975. Abnormal formation pressure. AAPG Bull. 59, 957–973.
Brunstrom, R.G.W., 1963. Recently discovered oil fields in Britain. In: Proc—World Pet. Congr. 6, Sect. 1, Pap. 49, pp. 11–20.
Buckley, S.E., Hocutt, C.R., Taggart, M.S., 1958. Distribution of dissolved hydrocarbons in subsurface waters. In: Weeks, L.G. (Ed.), The Habitat of Oil. Am. Assoc. Pet. Geol., Tulsa, OK, pp. 850–882.
Capuano, R.M., 1993. Evidence of fluid flow in microfractures in geopressured shales. AAPG Bull. 77, 1303–1314.
Carstens, H., Finstad, K., 1981. Geothermal gradients of the northern North Sea basin, 59–62°N. In: Illing, L.V., Hobson, G.D. (Eds.), Petroleum Geology of the Continental Shelf of North West Europe. Heyden Press, London, pp. 152–161.
Cartwright, J.A., 1994. Episodic basin-wide hydrofracturing of overpressured Early Cenozoic mudrock sequences in the North Sea Basin. Mar. Pet. Geol. 11, 587–607.
Case, L.C., 1945. Exceptional Silurian brine near Bay City, Michigan. AAPG Bull. 29, 567–570.
Case, L.C., 1956. The contrast in initial and present application of the term "connate water." J. Pet. Technol. 8, 12.
Chiarelli, A., 1978. Hydrodynamic framework of eastern Algerian Sahara—influence on hydrocarbon occurrence. AAPG Bull. 62, 667–685.
Claypool, G.E., Love, A.H., Maugham, E.K., 1978. Organic geochemistry, incipient meta-morphism, and oil generation in black shale members of Phosphoria formation, western interior United States. AAPG Bull. 62, 98–120.
Collins, A.G., 1975. Geochemistry of Oilfield Waters. Elsevier, Amsterdam.
Combarnous, M., Aziz, K., 1970. Influence de la convection naturelle dan les reservoirs d'huille ou de gas. Rev. Inst. Pr. Pet. 25, 1335–1354.
Cooper, B.S., Coleman, S.H., Barnard, P.C., Butterworth, J.S., 1975. Palaeotemperatures in the northern North Sea basin. In: Woodland, A.W. (Ed.), Petroleum and the Continental Shelf of North West Europe, vol. I. Applied Science Publishers, London, pp. 487–492.
Cousteau, H., 1975. Classification hydrodynamiques des bassins sedimentaires. Proc. World Pet. Congr. 9 (2), 105–119.
De Sitter, L.V., 1947. Diagenesis of oilfield brines. AAPG Bull. 31, 2030–2040.
Dickey, P.A., 1966. Patterns of chemical composition in deep subsurface waters. AAPG Bull. 50, 2472–2478.
Dickey, P.A., 1969. Increasing concentration of subsurface brines with depth. Chem. Geol. 4, 361–370.
Dickey, P.A., 1979. Petroleum Development Geology. Petroleum Publishing Co., Tulsa, OK.
Dickey, P.A., Cox, W.C., 1977. Oil and gas in reservoirs with subnormal pressures. AAPG Bull. 61, 2134–2142.
Downey, J.S., 1984. Geohydrology of the Madison and Associated Aquifers in Parts of Montana, North Dakota, South Dakota, and Wyoming. U.S. Geological Survey Professional Paper 1273-G, 47 p.
Dmitriyevsky, A.N., 1993. Hydrothermal origin of oil and gas reservoirs in basement rocks of the south Vietnamese continental shelf. Int. Geol. Rev. 35, 621–630.
Evans, T.R., 1977. Thermal properties of North Sea rocks. Log Analyst 18 (2), 3–12.
Fertl, W.H., 1977. Shale density studies and their application. In: Hobson, G.D. (Ed.), Developments in Petroleum Geology, vol. 1. Applied Science Publishers, London, pp. 293–328.
Fertl, W.H., Chilingarian, G.V., 1976. Importance of abnormal pressures to the oil industry. Soc. Pet. Eng. Pap. 5946, 1–11.
Fertl, W.H., Wichmann, P.A., 1977. How to determine static BHT from well log data. World Oil 184 (1), 105–106.
Friedman, G.M., Sanders, J.E., 1978. Principles of Sedimentology. Wiley, New York.
Hottman, C.E., Johnson, R.K., June 17, 1965. Estimation of formation pressures from log-derived shale properties. J. Pet. Technol. 717–722.
Hubbert, M.K., 1953. Entrapment of petroleum under hydrodynamic conditions. AAPG Bull. 37, 1954–2026.
Hubbert, M.K., Rubey, W.W., 1959. Role of fluid pressure in mechanics of overthrust faulting. AAPG Bull. 70, 115–166.
Hunt, J.M., 1996. Petroleum Geochemistry and Geology, second ed. Freeman, San Francisco.
Hunt, J.M., 1990. Generation and migration of petroleum from abnormally pressured fluid compartments. AAPG Bull. 74, 1–12.
Jacquin, C., Poulet, M., 1973. Essai de restitution des conditions hydrodynamiques regnant dans un basin sedimentaire au cours de son évolution. Rev. Inst. Fr. Pet. 28, 269–298.
Jones, P.H., 1969. Hydrodynamics of geopressure in the northern Gulf of Mexico basin. J. Pet. Technol. 21, 803–810.